

การแยกไอออน/อนุภาคระดับนาโนเมตรของเงินและทองในน้ำโดยใช้ซิลิกาตัดแปรทางเคมีสำหรับการ
ตรวจวัดเชิงสเปกโทรเมตรี



นางสาวพิมพ์พิมพ์ อเนกธีรกุล

บทคัดย่อและแฟ้มข้อมูลฉบับเต็มของวิทยานิพนธ์ตั้งแต่ปีการศึกษา 2554 ที่ให้บริการในคลังปัญญาจุฬาฯ (CUIR)
เป็นแฟ้มข้อมูลของนิสิตเจ้าของวิทยานิพนธ์ ที่ส่งผ่านทางบัณฑิตวิทยาลัย

The abstract and full text of theses from the academic year 2011 in Chulalongkorn University Intellectual Repository (CUIR)
are the thesis authors' files submitted through the University Graduate School.

วิทยานิพนธ์นี้เป็นส่วนหนึ่งของการศึกษาตามหลักสูตรปริญญาวิทยาศาสตรดุษฎีบัณฑิต

สาขาวิชาเคมี ภาควิชาเคมี

คณะวิทยาศาสตร์ จุฬาลงกรณ์มหาวิทยาลัย

ปีการศึกษา 2560

ลิขสิทธิ์ของจุฬาลงกรณ์มหาวิทยาลัย

SEPARATION OF SILVER AND GOLD IONS/NANOPARTICLES IN WATER USING
CHEMICALLY MODIFIED-SILICA FOR SPECTROMETRIC DETECTION

Miss Pimpimon Anekthirakun



A Dissertation Submitted in Partial Fulfillment of the Requirements
for the Degree of Doctor of Philosophy Program in Chemistry

Department of Chemistry

Faculty of Science

Chulalongkorn University

Academic Year 2017

Copyright of Chulalongkorn University

Thesis Title	SEPARATION OF SILVER AND GOLD IONS/NANOPARTICLES IN WATER USING CHEMICALLY MODIFIED-SILICA FOR SPECTROMETRIC DETECTION
By	Miss Pimpimon Anekthirakun
Field of Study	Chemistry
Thesis Advisor	Associate Professor Apichat Imyim, Ph.D.

Accepted by the Faculty of Science, Chulalongkorn University in Partial Fulfillment of the Requirements for the Doctoral Degree

.....Dean of the Faculty of Science
(Professor Polkit Sangvanich, Ph.D.)

THESIS COMMITTEE

.....Chairman
(Associate Professor Vudhichai Parasuk, Ph.D.)

.....Thesis Advisor
(Associate Professor Apichat Imyim, Ph.D.)

.....Examiner
(Professor Thawatchai Tuntulani, Ph.D.)

.....Examiner
(Associate Professor Narong Praphairaksit, Ph.D.)

.....External Examiner
(Associate Professor Tunlawit Satapanajaru, Ph.D.)

พิมพ์พิมล อเนกธีรกุล : การแยกไอออน/อนุภาคระดับนาโนเมตรของเงินและทองในน้ำโดยใช้ซิลิกาตัดแปรทางเคมีสำหรับการตรวจวัดเชิงสเปกโทรเมตรี (SEPARATION OF SILVER AND GOLD IONS/NANOPARTICLES IN WATER USING CHEMICALLY MODIFIED-SILICA FOR SPECTROMETRIC DETECTION) อ.ที่ปริกษาวิทยานิพนธ์หลัก: รศ. ดร. อภิชาติ อิ่มยิ้ม, 91 หน้า.

ศึกษาการแยกและตรวจวัดไอออน/อนุภาคระดับนาโนเมตรของเงินและทองในน้ำโดยใช้ซิลิกาที่ไม่ได้ทำการตัดแปรและตัดแปรทางเคมี ด้วยวิธีการสกัดด้วยเฟสของแข็งและวิเคราะห์เชิงปริมาณด้วยวิธีอินดักทีฟฟลูออโรสเปกโทรเมตรี (ICP-OES) ทำการเตรียมเฟสของแข็งโดยการตัดแปรอะมิโนโพรพิลซิลิกาด้วยของเหลวไอออนิกชนิด 1-carboxymethyl-3-methylimidazolium chloride ionic liquid [MimCM]Cl และกรดฮิวมิก ตัวดูดซับของแข็งอะมิโนโพรพิลซิลิกาที่ตัดแปรทางเคมีด้วยของเหลวไอออนิกใช้สำหรับการแยกไอออนและอนุภาคระดับนาโนเมตรของทอง ในขณะที่ตัวดูดซับของแข็งอะมิโนโพรพิลซิลิกาที่ตัดแปรด้วยกรดฮิวมิกใช้สำหรับการแยกไอออนและอนุภาคระดับนาโนเมตรของเงิน โดยการแยกเกิดจากตัวดูดซับของแข็งที่มีความเหมาะสมต่อการดูดซับกับไอออนโลหะมากกว่าอนุภาคระดับนาโนเมตรของโลหะ ดังนั้นจึงสามารถตรวจพบอนุภาคระดับนาโนเมตรของโลหะที่เหลืออยู่ในสารละลาย ทำการศึกษาหาภาวะที่เหมาะสมในการแยก ได้แก่ ค่าพีเอช เวลาในการสกัดแยก และชนิดของตัวชะ พบว่าพีเอช 3 เหมาะสมต่อการสกัดแยกไอออน/อนุภาคระดับนาโนเมตรของโลหะสำหรับตัวดูดซับของแข็งทุกชนิด ไอออนและอนุภาคระดับนาโนเมตรของทองใช้เวลาในการสกัดแยกที่เหมาะสม 5 นาที ในขณะที่ไอออนและอนุภาคระดับนาโนเมตรของเงินใช้เวลาในการสกัดแยก 15 นาที การศึกษาชนิดของตัวชะพบว่าไทโอยูเรียเป็นตัวชะที่เหมาะสมสำหรับตัวดูดซับอะมิโนโพรพิลซิลิกาที่ตัดแปรทางเคมีด้วยของเหลวไอออนิกและตัวดูดซับของแข็งอะมิโนโพรพิลซิลิกา สำหรับกรดไนตริกให้ประสิทธิภาพในการชะสูงสำหรับตัวดูดซับอะมิโนโพรพิลซิลิกาที่ตัดแปรด้วยกรดฮิวมิก จากการทดลองภายใต้ภาวะที่เหมาะสมพบว่า วิธีการนี้สามารถประยุกต์ใช้สำหรับการแยกไอออน/อนุภาคระดับนาโนเมตรของเงินและทองในผลิตภัณฑ์ที่ใช้ในครัวเรือนและตัวอย่างน้ำเสียจริง และตรวจวัดปริมาณด้วยวิธี ICP-OES โดยค่าเปอร์เซ็นต์การได้กลับคืนในการวิเคราะห์ไอออน/อนุภาคระดับนาโนเมตรของเงินและทองมีค่ามากกว่า 80% ค่าความเที่ยงในการวิเคราะห์ทั้งหมด (%RSD) ต่ำกว่า 3 และขีดจำกัดการตรวจวัดด้วยวิธี ICP-OES มีค่า 5.77 และ 4.61 ไมโครกรัมต่อลิตร สำหรับโลหะทองและเงินตามลำดับ

ภาควิชา เคมี ลายมือชื่อนิสิต

สาขาวิชา เคมี ลายมือชื่อ อ.ที่ปรึกษาหลัก

ปีการศึกษา 2560

5572829723 : MAJOR CHEMISTRY

KEYWORDS: SEPARATION / SILVER IONS / SILVER NANOPARTICLES / GOLD IONS / GOLD NANOPARTICLES / HUMIC ACIDS / IONIC LIQUIDS / MODIFIED-SILICA / ICP-OES

PIMPIMON ANEKTHIRAKUN: SEPARATION OF SILVER AND GOLD IONS/NANOPARTICLES IN WATER USING CHEMICALLY MODIFIED-SILICA FOR SPECTROMETRIC DETECTION. ADVISOR: ASSOC. PROF. APICHAT IMYIM, Ph.D., 91 pp.

The separation of gold and silver ions/nanoparticles in water using chemically-modified silica and unmodified silica was investigated by solid-phase extraction (SPE) followed by the determination via inductively coupled plasma-optical emission spectrometry (ICP-OES). 1-Carboxymethyl-3-methylimidazolium chloride ionic liquid [MimCM]Cl and humic acid (HA) immobilized onto aminopropyl silica (SiAP) sorbents were successfully prepared for the separation of metal species. Ionic liquid modified-SiAP (SiAP-IL) sorbent was chosen for the separation of gold ions/nanoparticles, while humic acids modified-SiAP (SiAP-HA) sorbent was selected for silver ions/nanoparticles. Based on this proposed method, the metal ions were preferentially adsorbed onto the solid sorbent over the metal nanoparticles, thus the metal nanoparticles were retained and observed in solution. The pH of solution, extraction time and types of eluent were optimized. The separation of metal species was observed at pH 3 for all adsorbents. The optimal extraction time of gold ions/nanoparticles was achieved within 5 minutes whereas a good separation of silver ions/nanoparticles was observed within 15 minutes. The higher elution efficiency of thiourea was observed for SiAP-IL and sequential elution of SiAP sorbent. Meanwhile, nitric acid showed high elution efficiency for SiAP-HA sorbent. Under the optimum conditions, the proposed method was successfully applied for the separation and determination of gold and silver species in household products and wastewater samples using ICP-OES. The recoveries of gold and silver ions/nanoparticles were higher than 80%. The overall %RSD are lower than 3. The detection limit (LOD) was 5.77 and 4.61 $\mu\text{g L}^{-1}$ for gold and silver, respectively, using ICP-OES.

Department: Chemistry

Student's Signature

Field of Study: Chemistry

Advisor's Signature

Academic Year: 2017

ACKNOWLEDGEMENTS

I would like to express my gratitude to all those who made the completion of this thesis possible. First of all, I would like to convey my gratitude to my advisor Associate Professor Dr. Apichat Imyim for his suggestions, assistance, constructive criticism, inspiration, encouragement, and strong support throughout the duration of my thesis. I am deeply appreciated to his guidance, patience and all the help he rendered me during times of research as well as accomplishment write up for this thesis. In addition, I would like to extend my appreciation to the members of my thesis committee; thanks to Associate Professor Dr. Vudhichai Parasuk, Professor Dr. Thawatchai Tuntalani, Associate Professor Dr. Narong Praphairaksit and Associate Professor Dr. Tunlawit Satapanajaru for all their valuable hints, corrections, and offered suggestions for my research improvement.

This work could not be completed without kindness and assistance of many people. I am particularly grateful to Assistant Professor Dr. Fuanfa Unob and Associate Professor Dr. Wanlapa Aeungmaitrepirom for their suggestions to solve problems that I encountered during my research. Furthermore, I would like to thank all my colleagues in the Environmental Analysis Research Unit (EARU). I treasure their friendship and their encouragement is what kept me going. The success of this research can be attributed to the Environmental Analysis Research Unit (EARU). This work was financially supported by the CU Graduate School Thesis Grant, Chulalongkorn University.

Finally, I would like to send a heartfelt acknowledgement to my family for the education, understanding, love, care, support, and especially for the encouragement they provided me throughout my study.

CONTENTS

	Page
THAI ABSTRACT	iv
ENGLISH ABSTRACT	v
ACKNOWLEDGEMENTS	vi
CONTENTS	vii
LIST OF TABLES	xii
LIST OF FIGURES	xiii
LIST OF ABBREVIATIONS	xv
CHAPTER I INTRODUCTION.....	1
1.1 Statement of the problem.....	1
1.2 Objective.....	3
1.3 Scope of the research.....	3
1.4 Benefit of this research.....	3
CHAPTER II THEORY AND LITERATURE REVIEW	4
2.1 Gold and gold nanoparticles.....	4
2.2 Silver and silver nanoparticles.....	5
2.3 Separation method of metal ions/nanoparticles	6
2.3.1 Ultrafiltration and ultracentrifugation.....	6
2.3.2 Chromatographic and electrophoretic separation.....	6
2.3.3 Solid-phase extraction	7
2.3.4 Liquid-phase extraction.....	8
2.3.5 Cloud point extraction.....	8
2.4 Solid-phase extraction.....	8

	Page
2.4.1 Theory and basic principles of SPE.....	9
2.4.2 Solid-phase extraction procedure.....	10
2.5 Chemically modified-silica gel.....	10
2.6 Ionic liquids	11
2.6.1 Background and characteristics.....	11
2.7 Humic acids	14
2.7.1 Background and characteristics.....	14
2.7.2 Binding ability of humic acid on metals.....	15
2.8 Literature review on speciation analysis of metal ions and nanoparticles.....	15
CHAPTER III EXPERIMENTAL.....	20
3.1 Chemical	20
3.2 Instruments.....	21
3.3 Preparation of gold nanoparticles (AuNPs).....	22
3.3.1 Preparation of reducing reagent	22
3.3.2 Preparation of stabilizer.....	23
3.3.3 Preparation of AuNPs	23
3.4 Preparation of silver nanoparticles (AgNPs).....	24
3.4.1 Preparation of AgNPs using starch stabilizer	24
3.4.2 Preparation of AgNPs using citrate stabilizer.....	24
3.5 Preparation of aminopropyl silica (SiAP)	24
3.6 Synthesis of 1-carboxymethyl-3-methylimidazolium chloride ionic liquid, [MimCM]Cl	25
3.7 Immobilization of [MimCM]Cl onto SiAP	25

	Page
3.8 Immobilization of HA onto SiAP.....	25
3.9 Optimization of Au and Ag ions/nanoparticles extraction.....	26
3.9.1 Effect of pH.....	26
3.9.2 Effect of time.....	26
3.9.3 Adsorption isotherm.....	27
3.10 Separation of metal ions/nanoparticles.....	27
3.11 Elution procedure.....	27
3.12 Sequential elution procedure.....	28
3.13 Method validation.....	28
3.13.1 Accuracy and precision.....	29
3.13.2 Limit of detection (LOD).....	29
CHAPTER IV RESULTS AND DISCUSSION.....	30
4.1 Characterization of SiAP-IL.....	30
4.1.1 Fourier transform infrared spectroscopy (FT-IR).....	30
4.1.2 Surface area analysis.....	31
4.2 Gold nanoparticles.....	32
4.3 Optimization of Au ions/nanoparticles extraction.....	35
4.3.1 Effect of pH.....	35
4.3.2 Effect of time.....	38
4.4 Adsorption isotherm of Au(III).....	41
4.5 Separation of Au ions/nanoparticles.....	44
4.6 Method validation.....	48
4.7 Characterization of SiAP-HA.....	52

	Page
4.7.1 Fourier transform infrared spectroscopy (FT-IR)	53
4.7.2 Surface area analysis	53
4.7.3 DR-UV-Vis	54
4.8 Silver nanoparticles	55
4.9 Optimization of Ag ions/nanoparticles extraction	56
4.9.1 Effect of pH	56
4.9.2 Effect of time	58
4.10 Adsorption isotherm of Ag(I)	58
4.11 Separation of Ag ions/nanoparticles	60
4.12 Method validation	64
4.13 Characterization of SiAP	65
4.13.1 Fourier transform infrared spectroscopy (FT-IR)	65
4.13.2 Surface area analysis	66
4.14 Optimization of Ag ions/nanoparticles extraction	67
4.14.1 Effect of pH	67
4.14.2 Effect of time	67
4.15 Adsorption isotherm of Ag(I) and AgNPs	68
4.16 Sequential elution of Ag(I) and AgNPs	71
4.17 Method validation	74
CHARTER V CONCLUSION	76
5.1 Conclusion	76
5.2 Suggestions for future work	77
REFERENCES	78

VITA..... 91



จุฬาลงกรณ์มหาวิทยาลัย
CHULALONGKORN UNIVERSITY

LIST OF TABLES

Table	Page
2.2 Ionic liquids modified silica sorbent.....	13
3.1 List of chemicals.....	20
3.2 List of instruments.....	21
3.3 ICP-OES conditions for the determination of silver and gold ions/nanoparticles..	22
4.1 Summary of the adsorbent parameters measured by surface area analysis.....	32
4.2 Analytical result of Au(III) ions and AuNPs in sample (n=3).....	49
4.3 Summary of the adsorbent parameters measured by surface area analysis.....	54
4.4 Analytical results of Ag(I) ions and AgNPs in sample (n=3).....	64
4.5 Detection limit (LOD) of the proposed method.....	65
4.6 Summary of the adsorbent parameters measured by surface area analysis.....	66
4.7 Analytical results of Ag(I) ions and AgNPs in sample (n=3).....	74
4.8 Analyte recovery and precision at different concentration [99].....	75

LIST OF FIGURES

Figure	Page
2.1 Solid phase extraction procedure [45].....	10
2.2 The schematic representation of chemically modification of silica surface.....	11
2.3 Structure of cations in ionic liquids.....	12
2.4 Structure of anions in ionic liquids.....	12
2.5 Model structure of humic acid [67].....	15
4.1 Schematic representation of the immobilization between SiAP and [MimCM]Cl.....	30
4.2 FT-IR spectra of aminopropyl silica (SiAP), [MimCM]Cl ionic liquid and [MimCM]Cl ionic liquid modified-aminopropyl silica (SiAP-IL).....	31
4.3 Visible spectrum of gold nanoparticles.....	33
4.4 UV-Vis spectrum of AuNPs in aqueous solution with different diameter size [83].....	33
4.5 TEM images (300,000 × magnification) of (a) non-stabilizer AuNPs (b) citrate-AuNPs and (c) starch-AuNPs.....	34
4.6 Effect of pH on the extraction of Au(III) by SiAP and SiAP-IL.....	35
4.7 Effect of pH on the extraction of AuNPs by SiAP-IL.....	36
4.8 Schematic representations of various types of stabilizer immobilized-AuNPs (a) tri-sodium citrate (b) starch and (c) CTAB.....	37
4.9 Effect of extraction time on the extraction of Au(III) using SiAP-IL.....	39
4.10 Effect of extraction time on the extraction of AuNPs using SiAP-IL.....	41
4.11 Langmuir isotherm of Au(III) onto SiAP-IL.....	42
4.12 Freundlich isotherm of Au(III) onto SiAP-IL.....	43

4.13 Adsorption isotherm of Au(III) onto SiAP-IL.....	43
4.14 The recovery of AuNPs by SiAP-IL.....	45
4.15 Elution of Au(III) ions using 0.1M HNO ₃ , 0.1M H ₂ SO ₄ and 0.1M thiourea as eluents.....	47
4.16 Schematic representation of HA immobilized onto SiAP.....	52
4.17 FT-IR spectra of aminopropyl silica (SiAP), humic acid (HA) and HA immobilized on aminopropyl silica (SiAP-HA).	53
4.18 DR-UV-Vis spectra of SiAP and SiAP-HA.....	54
4.19 TEM images (150,000 × magnification) of (a) starch-AgNPs and (b) citrate-AgNPs.	55
4.20 Effect of pH on the extraction of Ag(I) and AgNPs by SiAP-HA.	56
4.21 Effect of pH on the extraction of Ag(I) and AgNPs by SiAP.....	57
4.22 Effect of extraction time on the extraction of Ag(I) and AgNPs by SiAP-HA.....	58
4.23 Langmuir isotherm of Ag(I) onto SiAP-HA.	59
4.24 Freundlich isotherm of Ag(I) onto SiAP-HA.....	59
4.25 Adsorption isotherm of Ag(I) onto SiAP-HA.....	60
4.26 Schematic representations various types of stabilizer immobilized-AuNPs (a) starch and (b) tri-sodium citrate.....	61
4.27 The recovery of starch stabilized-AgNPs by SiAP-HA.	61
4.28 The recovery of tri-sodium citrate stabilized-AgNPs by SiAP-HA.....	62
4.29 Elution of Ag(I) ions in the existence of starch-AgNPs using 0.1 M HNO ₃ , 0.1 M H ₂ SO ₄ and 0.1 M Thiourea as eluents.....	63
4.30 Elution of Ag(I) ions in the existence of citrate-AgNPs using 0.1 M HNO ₃ , 0.1 M H ₂ SO ₄ and 0.1 M Thiourea as eluents.....	63
4.31 Schematic representation of SiAP synthesis.....	65

4.32 FT-IR spectra of silica gel and aminopropyl silica (SiAP).	66
4.33 Effect of extraction time of Ag and AgNPs at pH 3 by SiAP.	68
4.34 Langmuir isotherm of Ag(I) and AgNPs onto SiAP.	69
4.35 Freundlich isotherm of Ag(I) and AgNPs onto SiAP.....	70
4.36 Adsorption isotherm of Ag(I) and AgNPs onto SiAP.	71
4.37 Elution of Ag(I) and AgNPs by varying eluents (0.1M HNO ₃ , 0.1M H ₂ SO ₄ and	73



LIST OF ABBREVIATIONS

ICP-OES	=	Inductively coupled plasma-optical emission spectrometry
FT-IR	=	Fourier transform infrared spectrometry
UV-Vis	=	Ultraviolet visible spectrometry
DR-UV-Vis	=	Diffuse reflectance ultraviolet visible spectrometry
SPR	=	Surface plasmon resonance
MNPs	=	Metal nanoparticles
AuNPs	=	Gold nanoparticles
AgNPs	=	Silver nanoparticles
AgNSs	=	Silver nanospheres
SiAP	=	Aminopropyl silica
HA	=	Humic acid
IL	=	Ionic liquid
LOD	=	Limit of detection
°C	=	Degree Celsius
s	=	Second
µm	=	Micrometer
nm	=	Nanometer
µg	=	Microgram
mg	=	Milligram
g	=	Gram
L	=	Litre
mL	=	Millilitre
M	=	Molar
mM	=	Millimolar
v/v	=	Volume by volume
w/v	=	Weight by volume
rpm	=	Revolutions per minutes

CHAPTER I

INTRODUCTION

1.1 Statement of the problem

Metal ions and metal nanoparticles (M-NPs) are widely used in various applications such as electrical appliances, pharmaceutical production, and industrial process applications. However, nanosized materials are interesting matters due to their properties such as the unique physicochemical property, high surface-to-volume ratio, and durability [1-3]. Especially for silver nanoparticles (AgNPs) and gold nanoparticles (AuNPs), they are commonly used in consumer products including textiles, medical devices, water filters, paints, electrical devices, and food industries. The increasing of M-NPs utilization leads to arising of their release in environment and tends to adversely impact on a variety of organisms including plants, fishes, and human cell [4]. M-NPs are reported that they display high toxicity in comparison to metal ion species of the same element [5]. Furthermore, The United States Environmental Protection Agency (EPA) comprehensively regulated for nanomaterial manufacture, which is reported unusual properties different than the same element, in order to protect the risk to environment and human health [6-8]. Therefore, it is necessary to study the effective method to separate and determine metal ions and M-NPs.

A number of studies have been focused on the separation of silver and gold ions and their nanoparticles prior to detection with desired methods such as ultrafiltration and ultracentrifugation for the preconcentration and purification of nanoparticles (NPs), hydrodynamic chromatography (HDC) coupled with single-particles inductively coupled plasma mass spectrometry (SP-ICP-MS) used for the separation of NPs on the basis of isolating particle size due to flow rate velocity gradient, micellar electrokinetic chromatography (MEKC) coupled with ICP-MS, reversed-phased liquid chromatography (RP-LC) combined with ICP-MS, cloud point extraction followed by electrothermal atomic adsorption spectrometry, ion selective

electrode (ISE), and liquid phase extraction [9-17]. However, proficiency and expensive operation are required for these techniques.

Solid phase extraction (SPE) is an alternative method for extraction of metals. Many researchers have investigated on finding low-cost as well as environmental friendly sorbents [18, 19]. Room temperature ionic liquids (ILs) are environmental friendly organic salts which have been greatly selected in various chemistry fields due to some unique properties such as high thermal stability, non-volatility and non-flammability [20]. Their properties can be controlled by changing cations or anions functional groups and employed as solvent media for metal ions separation [21]. Therefore, they have been used in various applications such as solvent extraction, solid-phase extraction, liquid chromatography, electrochemistry and spectroscopy [22-24]. Another environmental friendly organic matter is humic acids (HA) which are defined as organic matters and usually available in nature which is found in soil, slime, and rotten vegetable [25]. They are interesting materials which contained various functional groups such as carboxylic, phenolic, and hydroxyl group that are responsible for the adsorption of heavy metals [26, 27]. However, the obstacle in application of these two materials for metal ions extraction is higher viscosity of ILs which probably cause long time for equilibration, low mass transfer rate and difficult phase isolation. Immobilization of ILs and HA onto a solid support can improve the efficiency and overcome these limitation. Among various types of solid support, modified silica gel is an interesting material due to its large specific area and good thermal stability. Nevertheless, there are insufficient studies on applying ILs and HA onto a solid sorbent for the extraction and determination of Au and Ag ions/nanoparticles. Thus in this work, SiAP sorbent, ILs modified-aminopropyl silica (SiAP-ILs) and HA modified-aminopropyl silica (SiAP-HA) were prepared and applied for separation of Au and Ag ions/nanoparticles in aqueous solution and their concentrations were measured by inductively coupled plasma-optical emission spectrometry (ICP-OES).

1.2 Objective

The objective of this research is (1) to synthesize modified-silica with ionic liquids and humic acids and (2) to separate gold and silver ions/nanoparticles in aqueous solution using chemically modified-silica for measurement by ICP-OES.

1.3 Scope of the research

The scope of this research include the modification of aminopropyl silica (SiAP) by 1-carboxymethyl-3-methylimidazolium chloride ionic liquid ([MimCM]Cl) and humic acids (HA). The modified-silica was applied for the extraction of Au and Ag ions/nanoparticles in aqueous solution. Factors affecting the extraction of metals such as pH of solution, extraction time and adsorption isotherm were investigated. Furthermore, elution study of metal ions was also studied by various eluents. The feasibility of this proposed method was studied by method validation in real samples.

1.4 Benefit of this research

The effective modified-silica for separation and determination of Au and Ag ions/nanoparticles in aqueous solution was obtained.

CHAPTER II

THEORY AND LITERATURE REVIEW

2.1 Gold and gold nanoparticles

Gold (Au) is one of the most important precious metals that are widely applied in various industries, for instance, electrical systems, fuel cells, catalyst and biomedical fields due to its unique physical and chemical properties. As for gold nanoparticles (AuNPs), they have been applied in biomedical imaging, cancer therapy, biological and chemical sensing [28]. In case of diagnostics, the change of physicochemical properties as surface plasmon resonance of AuNPs is occurred after the binding of between analytes and metal nanoparticles (MNPs). This variation is depending on particles size, shape, surrounding or aggregation which leads to the color change of AuNPs. The utilization concept from this phenomenon is if there are any external stimuli presented, a colloidal solution of gold exhibits color change from red to purple or blue. In addition, they are applied in various target analytes such as heavy metal ions, DNA, protein and others. Nowadays, a versatile surface chemistry of gold nanoparticles allows them to be employed extensively in various applications. The most commonly used method for the preparation of AuNPs is the chemical reduction of Au(III) salt by using various reducing agents in the presence of a stabilizing agent that can allow chemisorption and/or physisorption on AuNPs surface to avoid their aggregation [29]. The reduction of hydrogen tetrachloroaurate (HAuCl_4) with citric acid in boiling water, where the citrate acts as reducing and stabilizing agent, has been widely employed to prepared moderately stable spherical gold nanoparticles with diameters of 10 to 20 nm [30]. The spherical AuNPs exhibit a range of color for instance red, purple, orange and brown in aqueous solution as the size in the range of 1 to 100 nm, and generally display a size-relative absorption peak around 500 to 550 nm [31].

2.2 Silver and silver nanoparticles

Silver (Ag) is considered metal that has a long history as disinfectant. Silver applications depend on their antimicrobial properties such as treat wounds and burns treatment. Silver nanoparticles (AgNPs) has been rapidly developed in various consumer products such as textiles, medical products, food containers, cosmetics, paints, socks, laundries and cleaners due to the fact that it was claimed as anti-bacterial and anti-fungal materials [32-34]. Moreover, some unique properties of AgNPs, for example, a high electrical and thermal conductivity, are being interested in microelectronic and medical imaging [1]. The surface plasmon resonance of Ag nanoparticles shows a unique strong absorption band in visible region which shows optical properties in strong yellow colloidal solution. Several physical and chemical techniques have been described for the synthesis of AgNPs. The techniques involve mechanically reducing bulk silver such as lithography or laser ablation. These methods tend to generate powders which provide less control of size and shape of the particles [1]. Other methods involve the dissolution of silver salts, such as silver nitrate into a solvent, followed by the addition of reducing agent and possibly supplemented by a stabilizing agent in order to prevent nanoparticle agglomeration [7]. The type of stabilizing agent has a significant effect on the surface changing behavior, particle size and the aggregation of AgNPs [35]. Moreover, biological reduction and green synthesis methods are of particular interest as they are less toxic and less cost than physical and chemical methods by utilizing micro-organisms and plant extracts [36].

However, the increasing use of metal ions and metal nanoparticles has given rise to their releasing into environment. This obviously affects to human and living things. For example, gold nanoparticles displayed adverse impact on human skin, lung and stem cells [37-39]. Furthermore, a number of studies have been focused on the toxicity of silver nanoparticles affecting to plants, fish and human cells [6, 40, 41]. Therefore, the simultaneous detection of metal nanoparticles and corresponding metal ions in samples is essential for quality control for products containing these nanoparticles and environmental pollution monitoring.

2.3 Separation method of metal ions/nanoparticles

2.3.1 Ultrafiltration and ultracentrifugation

The separation on the basis of molecular sizes is belonging to ultrafiltration techniques which used to separate nanoparticles (NPs). This technique enable to fraction, preconcentration and purification of NPs. The separation of NPs from the matrix occurs after hydrostatic force is applied on a membrane. Then, the retention of the lowest molecular weight, which 90 % of solute, is observed which defined as molecular weight cut-off (MWCO). Various membranes such as cellulose acetate, regenerated cellulose and polysulfone have been employed for NPs separation. The membrane with MWCO of 10-100 kDa is reported to separate NPs with diameter ranging 1-5 nm [13, 37].

Another technique involving the separation of NPs from solution by sedimentation is ultracentrifugation. The efficiency of this technique is depending on the applied force and centrifugation time. A higher centrifugation force and longer time are essential for stable removal of small particle sizes from aqueous medium. This method is suitable for preconcentration, purification and determination of the sediment phase and ions in the supernatant. The sufficient for separation of ultracentrifugation at 13000 rpm for 10 min is reported for the average size of NPs ranging of 10-30 nm. However, the NPs may retained in the supernatant after ultracentrifugation and probably result in NPs aggregation instead of the use of high ultracentrifugation force applied [14, 38].

2.3.2 Chromatographic and electrophoretic separation

Nanoparticles separation by chromatographic method such as hydrodynamic chromatography (HDC) is relied on the basis of separating particles due to a flow velocity gradient in a capillary column packed with nonporous microparticles. Various types of HDS such as open-tubular capillary and packed beds microchip have been selected for separation. Capability of HDC for particles

separation is size ranging between 5 and 1200 nm. It has been usually coupled with single-particle inductively coupled plasma mass spectrometry (SP-ICP-MS). The other detectors, such as dynamic light scattering (DLS), ultraviolet-visible (UV-Vis) and fluorescence spectroscopy have been coupled with HDC. And another conventional chromatographic technique employed for NPs separation is reverse-phase liquid chromatography coupled with ICP-MS (RP-LC-ICP-MS) [11, 38].

The electrophoretic technique has been applied for NPs separation. Gel electrophoresis, isoelectric focusing (IEF) and capillary electrophoresis (CE) are methods commonly used for fractionation of NPs by applying electric field in capillary. The separation technique of gel electrophoresis is based on the different migration of analytes in gel under electric field. IEF is a routine technique used to examine the isocratic point of macromolecules and also applied to separate NPs. CE is electro-migration separation technique which has been employed in selective separation of NPs by size and surface-charge density. Various modification agents, mobile phase buffers, water-dispersed and charged nanoparticles have been used for separation due to the different of their electrophoretic mobilities and migration rate in capillary. However, micellar electrokinetic chromatography (MEKC) coupled with ICP-MS was employed for separation, characterization and species selective detection of NPs [10, 15].

2.3.3 Solid-phase extraction

Solid-phase extraction (SPE) is currently practical method for effectiveness sample preparation, especially for NPs. The noble metal nanoparticles such as silver, gold and palladium-NPs were successfully separated by anion-exchange resin due to electrostatic interaction between ammonium groups on the resin surface and carboxylate groups coated on NPs. However, longer time around 42 hours was needed to yield good recoveries [39]. The retention of gold nanoparticles was studied by using reverse phase C18 column prior to extract with dodecanethiol in chloroform under ultrasonication and measured by electrothermal atomic

absorption spectrometry (ET-AAS) [40]. Moreover, the use of magnetic SPE was extended to employ for separation of metal species [28].

2.3.4 Liquid-phase extraction

Extraction of water-soluble NPs into water and hydrophobic NPs into organic solvent has been studied for purification and separation of NPs. Accordingly, the partition coefficient and migration of NPs are mainly performed distribution in immiscible solvents. Moreover, the affinity of nanoparticle through solvent can be changed by various surface modifications [41].

2.3.5 Cloud point extraction

Cloud point extraction is the separation technique based on the solubility and cloud point of non-ionic surfactant. The extraction process is changing conditions of pH, temperature, pressure or ionic strength and then mixture becomes turbid. Centrifugation or long-term standing is required to separate two phase and analytes can be extracted into the surfactant phase due to the analyte-micelle interaction [42].

However, the selection of suitable technique is required for separation metal ions and nanoparticles. In practice, the main requirements for selection are ease of procedure, equipment, timing, personal skill and operation cost. Thus, solid-phase extraction is appropriate technique and optional method for metal ions/nanoparticles separation.

2.4 Solid-phase extraction

Solid –phase extraction (SPE) is the most widely used for sample preparation that has been achieved for the separation and preconcentration of analyte from sample matrix instead of liquid-liquid extraction (LLE). Many problems associated

with LLE such as incomplete phase extraction, lower quantitative recoveries, use of expensive, time consuming and excessive use of organic solvents.

SPE is generally used for the extraction of liquid samples and particularly for semivolatile, non-volatile analytes or solid sample that pre-extracted into solvent. Various types of materials employed as sorbent for SPE are useful for extraction, preconcentration and cleanup which depend on a wide variety of chemistry, adsorbents and sizes [23].

The selection of solid sorbent in SPE is important to accomplish separation and preconcentration process. The analytical parameters used to consider such as selectivity, affinity and capacity. Thus, the modification of classical SPE materials has been used for many methods to improve the selectivity [43].

2.4.1 Theory and basic principles of SPE

Distribution equilibrium is involving to solid-phase extraction procedure. The adsorption behavior on a solid sorbent is the partition of analytes between a liquid sample phase and a solid sorbent phase. When the extraction reaches equilibrium, the ratio of analytes remained in solution to those of adsorbed onto solid sorbent will shows a constant value that can be defined as the distribution coefficient, K_d [44] expressed in equation 2.1.

$$K_d = \frac{\text{analyte adsorbed on sorbent (mmol g}^{-1}\text{)}}{\text{analyte remained in solution (mmol mL}^{-1}\text{)}} \quad (2.1)$$

The K_d value is usually observed by batch method and have been reported for analytes on different sorbents and various solutions. If K_d is larger, an analyte can be strongly adsorbed on solid sorbent, while K_d is smaller, it tends to remain in the sample solution.

2.4.2 Solid-phase extraction procedure

A solid-phase extraction procedure is presented in Figure 2.1 for batch method.

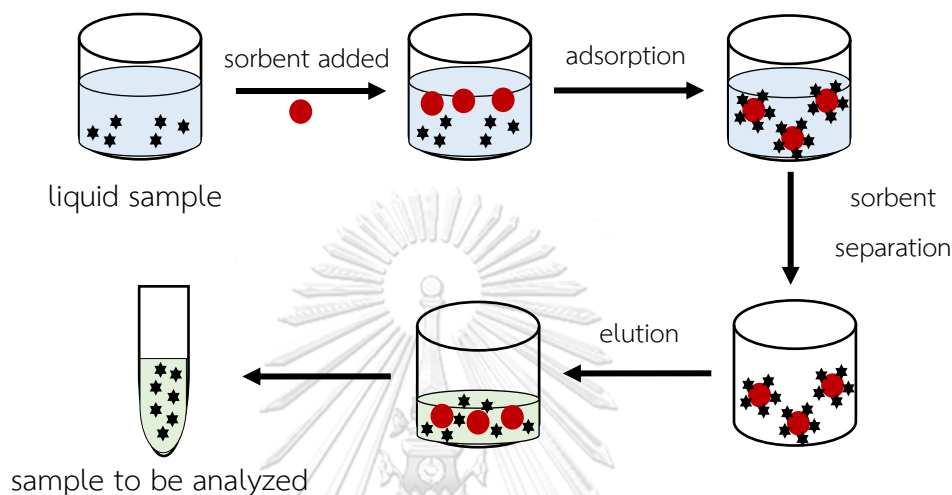


Figure 2.1 Solid phase extraction procedure [45].

In this procedure, solid sorbents are added to the solution containing analytes. They are adsorbed onto the adsorbent and then analytes are consequently eluted from the recover adsorbent prior to analyze with desired method. Moreover, the mechanism of elements in solid-phase extraction process is involved a simple adsorption (Van der Waals forces or hydrophobic interaction), chelation (metal-ligand interaction) or ion-exchange (electrostatic interaction).

2.5 Chemically modified-silica gel

Inorganic based sorbents are mainly produced from silica gel. They are demonstrating the advantages of mechanical, thermal and chemical stability under different conditions. The modification of silica gel surface is generally utilized via silanol groups. The chemically modification of silica gel has been developed in many applications such as chromatography, extraction of cations from aqueous and non-

aqueous solvents, removal of heavy metals from wastewater and also in catalytic reaction [46-49]. The silica gel surface is characterized by the presence of silanol groups which are weak ion-exchanger at higher pH range than 4, causing lower binding to ionic species [50]. This original silica gel has a very low selectivity and tends to hydrolysis at basic pH range. Thus, modification of silica gel surface is preferable to use with greater selectivity.

The silica surface composes of siloxane (Si-O-Si) and silanol (Si-OH) groups. The chemical modification can occur via the reaction with these functional groups. The organic functional groups that widely employed to modify with silica gel are 3-aminopropyltriethoxysilane [51, 52], 3-chloropropyltrimethoxysilane [53] and 3-mercaptopropyltrimethoxysilane [54]. The chemically modification of silica surface is shown in Figure 2.2.

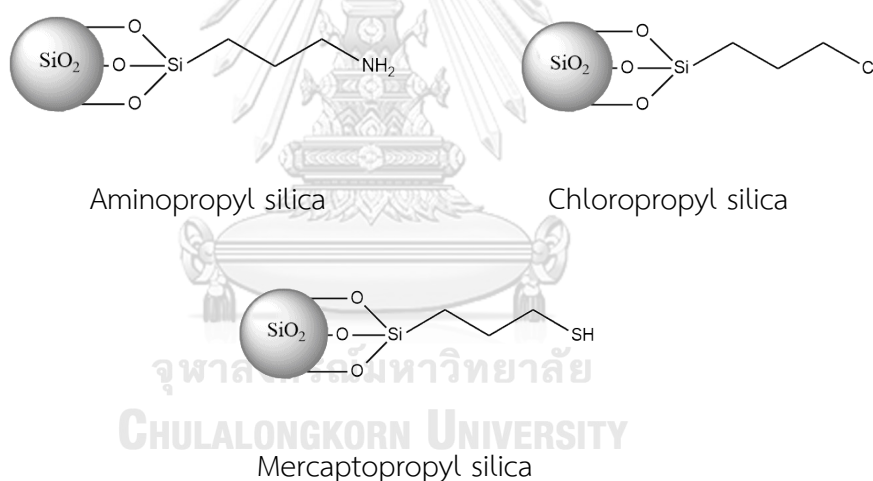


Figure 2.2 The schematic representation of chemically modification of silica surface.

2.6 Ionic liquids

2.6.1 Background and characteristics

Room temperature ionic liquids are organic salts with melting point lower or close to room temperature. They have unique and fascinating characteristics

such as high chemical and physical stability, trivial volatility, tunable viscosity and nonflammability [20]. Various properties of ionic liquids can be controlled by changing cations and anions in the structure [21]. Organic cations consist of imidazolium, pyrrolidinium, pyridinium, tetraalkyl ammonium or tetraalkyl phosphonium (Figure 2.3), while inorganic or organic anions comprises tetrafluoroborate, hexafluorophosphate, chloride, bromide or iodide (Figure 2.4). For this reason ionic liquids are generally known as designer solvents. They have commonly applied in different chemistry fields such as organic, inorganic, analytical and electrochemistry [22-24]. Especially use for environmental friendly solvent which can replace toxic volatile organic compounds.

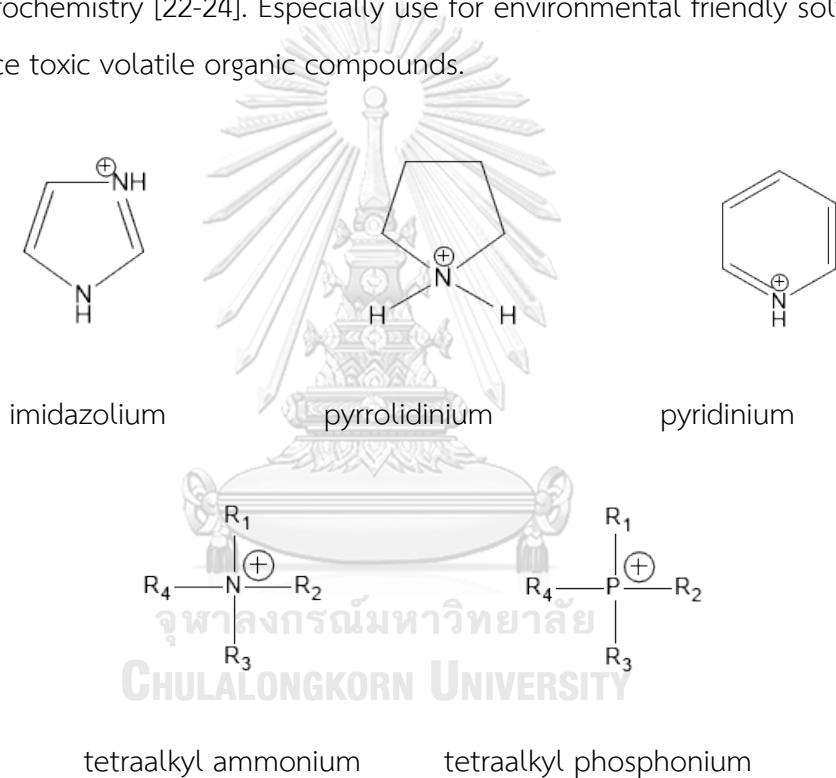


Figure 2.3 Structure of cations in ionic liquids.

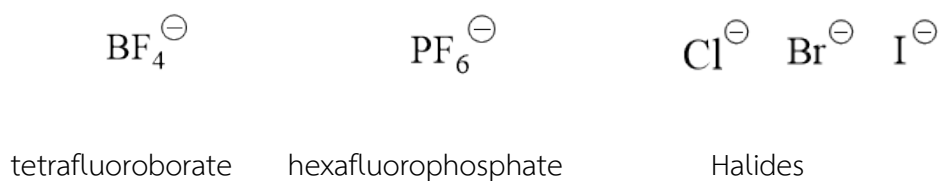
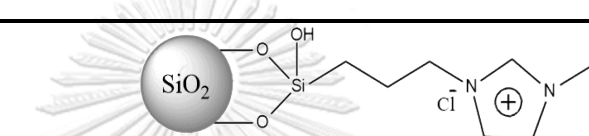
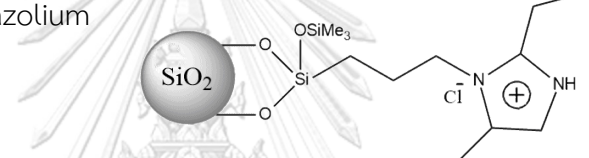
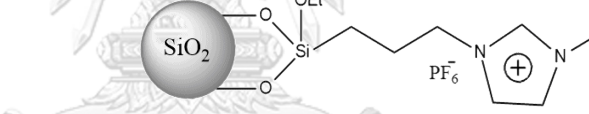
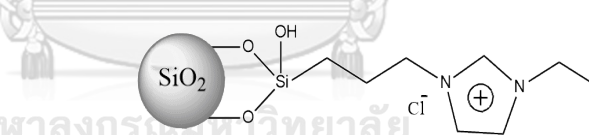
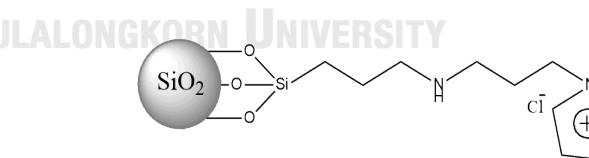


Figure 2.4 Structure of anions in ionic liquids.

Modification of classical SPE using immobilization of material surfaces are widely investigated such as silica with ionic liquids or polymerization of materials with ionic liquids. Ionic liquids have been commonly used in a SPE process to covalently attach to imidazole groups of silica surface [55, 56]. Many researchers have been carried out on solid-phase extraction studies with ionic liquid modified silica sorbents as shown in Table 2.1.

Table 2.1 Ionic liquids modified silica sorbent.

Ionic liquids	structure	Ref.
N-Methylimidazolium chloride		[57]
2-Ethyl-4-methylimidazolium chloride		[56]
N-Methylimidazolium hexafluorophosphate		[58]
N-(Propyl-3-sulfonate) imidazolium chloride		[22]
Imidazolium chloride		[59]

Although, the liquid state of ionic liquids are lost when they are covalently immobilized on the silica sorbent, other unique properties such as polarity and low volatility associated to non-polar and also ionic interactions are preserved [60]. The potential of these materials are low-polarity phase for non-polar compounds and attribute to the electrostatic and ion-exchange interaction between analyte and sorbent.

2.7 Humic acids

2.7.1 Background and characteristics

Humic acids (HAs) are macromolecules that compose of humic substance and commonly known as a portion of organic matter in soil. HAs are the fraction of humic substance that are soluble in basic medium, partially soluble in water and insoluble in acid and alcohol. However, this property was varied with the HAs composition, pH and ionic strength. They appear in rotting vegetable matter and can be observed in the black slime. They are obviously found in dark brown to black matters which depend on a variation of soils, peats, lignite, and brown coals. HAs are generally formed via microbiological decomposition and chemical degradation of plant tissues [25, 61, 62].

Various functional groups of HAs are mainly comprised carboxylic, phenolic and hydroxyl groups, and some functional groups of nitrogen, sulfur and phosphorus [63]. Nevertheless, HA surface contains mainly carboxyl functional groups which allow the deprotonation to carboxylate. Therefore, the negative charge of HAs under acidic conditions provides a high affinity of binding sites for metal ions in solution due to carboxylic groups that are responsible for weak acid behavior of HAs [64]. Different functional groups containing in HAs depend on the geographical origin, age, climate and environmental conditions. Molecular weights of HAs are in the range of 2.0 to 1300 kDa [65]. Their structure is composed of hydrophilic part of hydroxyl group and hydrophobic part of aliphatic chains as well as aromatic rings [66]. The humic acid structure is shown in Figure 2.5.

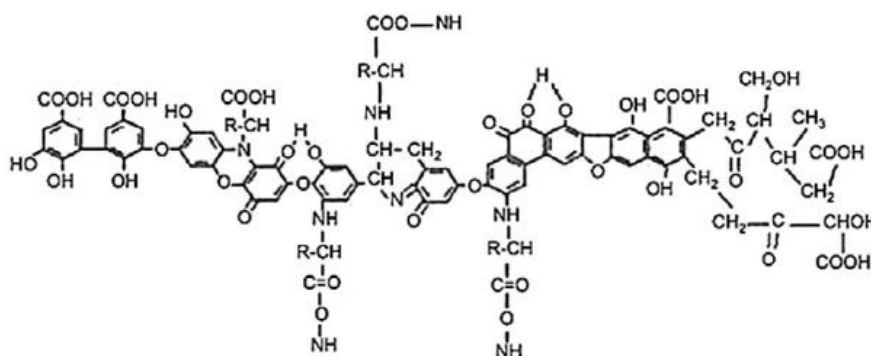


Figure 2.5 Model structure of humic acid [67].

2.7.2 Binding ability of humic acid on metals

The binding ability of HA to cationic metals make them profitable in various applications such as the removal of heavy metals in soil and water, the transport of micronutrients from soil to plant, the inhibition of the formation of free radicals by metal catalysis, reduction and stabilization of metal nanoparticles [68-70]. HAs molecules and metal cations exhibit initial entirely interaction for electrostatic and the cations move to their preferred location within HA structure [71, 72]. This ability enables their use as pollution treatment by removing heavy metal ions from water and soil.

2.8 Literature review on speciation analysis of metal ions and nanoparticles

The rapid advancement of nanotechnology over decades has influence on industrial process. For instance, Au nanoparticles have long been associated in biomedical imaging, cancer therapy and diagnostics, and electronic devices. Ag nanoparticles have also been used as anti-microbial and anti-fungal in household products, clothing, food containers, pharmaceuticals and electronics. Along with the development of nanomaterial technology, it has been realized that their release or residue could impact on human health, living things and environment. The nanoscale materials give new characteristic effect of optical property, morphology, high surface area to volume ratio, and durability. Moreover, they have been reported

that metal nanoparticles exhibited higher toxicity in comparison to metal ions form of the same element [5, 28]. In addition, The United States Environmental Protection Agency (EPA) comprehensively regulated for nanomaterial manufacture, which is reported unusual properties different than the same element, in order to protect the risk to environment and human health [6-8]. Therefore, it is necessary to study the effective method to separate and determine metal ions and metal nanoparticles in sample.

In 2008, Ngeontae et al. [9] have developed a new calix[4]arene containing benzothioazole groups, CU1, incorporated into the plasticized PVC membranes to determine metal ions using ion selective electrode (ISE). These Ag-ISEs were utilized for speciation analysis of silver nanoparticles (AgNPs). AgNPs solution was prepared from Ag(I) salt reduction. The residue of Ag ion could be observed after reduction of Ag(I) salt. Hence, the determination of Ag ions residue compared with total Ag ions concentration is crucial for the nanoparticle quantification. Moreover, these fabricated Ag-ISEs can be used in a wide range pH of 2-8 with response time less than 5 seconds. Thus, this fabricated electrode can be beneficial to researches regarding AgNPs.

Li et al. [39] studied an effective and selective method for metal nanoparticles in natural water by employing an anion exchange resin. Amberlite IRN-78 containing positive charges of ammonium groups was chosen in this study. Surface modification of metal nanoparticles (MNPs) was fabricated using mercaptosuccinic acid (MSA) and a bifunctional ligand. They were used to bind to metal nanoparticles surface through its thiol groups and two carboxylic functional groups were exposed to the medium. The MSA-modified MNPs were loaded onto resin directly in basic pH range ($\text{pH} > 7$), the electrostatic interaction between the positive charge of amino groups from resin and the negative charge of carboxylic groups from MSA ligands. With the proposed procedure, MNPs including gold, silver and palladium were selected for this study. Then, the element selective detection method of electrospray ionization (ESI) mass spectrometry was applied to quantify the present of MNPs. The recovery of Au, Ag, and Pd-NPs was obtained higher than 65 % with

regard to the low spike levels around 90-130 ng L⁻¹. Moreover, the enrichment factors of Au, Ag and Pd-NPs were 132, 138 and 163, respectively.

In 2012, Li and Leopold [40] considered for a new two-step extraction procedure of AuNPs from waters. Firstly, AuNPs containing in sample were loaded onto a reverse phase C-18 column (RP-C18) providing quantitative adsorption of AuNPs. The RP-C18 turns wine red in color of AuNPs at concentration higher than 1 mg L⁻¹. Then, the ligand-assisted extraction into chloroform was performed. 1-Dodecanethiol (1-DDT) was used as selective ligand for quantitative extraction incorporated with ultrasonic conditions at 0 °C. However, the RP-C18 loaded with AuNPs must be dried by application of vacuum prior to extract in the second step in order to improve the reproducibility. The optimized process provided a high enrichment factor of 250 and recoveries of 68.4-99.4 % that confirmed the feasibility of this approach. This characteristic of particles was proved by UV-Vis spectrometry and transmission electron microscopy (TEM).

A sequential analysis of AuNPs and Au ions in water was also investigated by combining magnetic solid-phase extraction. Su et al. [28] have applied Al³⁺ immobilized Fe₃O₄@SiO₂@iminodiacetic acid (IDA) for the extraction of AuNPs and Au ions. It was found that AuNPs and Au ions could be retained on this adsorbent. Then, their separation was achieved by sequential elution AuNPs and Au ions with Na₂S₂O₃ and NH₃.H₂O, respectively. The concentration of gold was quantified by inductively coupled plasma mass spectrometry (ICP-MS).

Lopez-garcia et al. [16] were evaluated the speciation of AgNPs and Ag ions by using a cloud point extraction (CPE) and the amount of metal was measured by electrothermal atomic absorption spectrometry. The Triton X-114 solution was chosen to extract AgNPs into a micellar phase after incubation at 40 °C for 10 minutes followed by centrifugation. Moreover, ammonium thiocyanate was incorporated in the sample solution to retain Ag ions in aqueous phase as well as prevent the extraction of Ag ions. Furthermore, Ramos et al. [3] were also focused on silver speciation. The migration of Ag ions from a commercial baby feeding bottle and plastic food containers were confirmed by scanning electron microscopy with energy dispersive X-ray (SEM-EDX) analysis. Silver release was observed at

temperature in the range of 20-70 °C using contact times of up to 10 days. As for AgNPs, single particle-inductively coupled plasma mass spectrometry (SP-ICP-MS) was employed to quantify AgNPs in the samples. Nevertheless, the use of an appropriate sample preparation procedure is required for this method of SP-ICP-MS to allow speciation of metals at ultra-trace level.

As mentioned, a solid-phase extraction is an optional method for separation and determination of metal ions and metal nanoparticles without any suitable sample preparation. Selectivity, easy to operate, low-cost and environmentally friendly adsorbent are priority selection. Thus, humic acids (HAs) and ionic liquids (ILs) are preferable for improvement of adsorbent selectivity.

Humic acids represent a large portion of natural organic matter in soils, sediments and waters. They are environmental friendly materials with strong complexation ability to heavy metals. Thus, several studies have focused on the interaction of metals with HAs in solution. Stathi et al. [73] were prepared three SiO₂-based materials via covalent immobilization of carboxyl groups (COOH), gallic acid (GA) containing phenolic groups and humic acids. Various heavy metals, for example Pb(II), Cd(II), Cu(II), Zn(II) and Mg(II), were used to evaluate the removal potential of prepared adsorbents. The adsorption capacity of the SiO₂-HA was 10 times higher than that of the other two materials. The concentration of metals, except Mg(II), was measured by anodic stripping voltammetry (ASV). The Mg(II) concentration was quantified by atomic absorption spectrometry (AAS). Moreover, Imyim et al. [74] were successfully prepared HA immobilized onto aminopropyl silica for simultaneously removal of heavy metals such as Ag(I), Cd(II), Cr(III), Ni(II), Pb(II) and Zn(II). The metal concentration was measured by flame atomic absorption spectrometry (FAAS). And the adsorption isotherm was fitted to the Langmuir model for all metal ions.

In addition, ionic liquids (ILs) have been considerably used as a green solvent. They have unique properties such as high thermal stability, negligible volatility, non-flammability, and modification of properties by selection of cations and anions. Tong et al. [75] was synthesized 1-hexadecyl-3-methylimidazolium chloride ionic liquids, [C₁₆mim]Cl, in chloroform system. They was employed for Au(III) extraction. The anion-exchange mechanism of Au(III) extraction by [C₁₆mim]Cl was monitored via UV-

Vis and FT-IR. Accordingly, the extracted mechanism is likely to be $[C_{16}mim]^+AuCl_4^-$. Wei et al. [76] was employed ionic liquid Aliquat-336 for a selective extraction of Au(III) from tertiary metal solution containing Au(III), Pt(IV) and Pd(II). Notably, Aliquat-336 was a very fast and effective extractant in liquid-liquid extraction (LLE) for selective extraction of Au(III) from multi-metal solution. However, the complexity of phase isolation was occurred in LLE. This limitation could be overcome by immobilization of ILs onto solid sorbent. Pu et al. [77] successfully prepared 1-carboxyethyl-3-methyl imidazolium hexafluorophosphate ionic liquids assembled onto silica wafers. Marwani et al. [78] was developed ionic liquid loaded amine silica gel for a selective extraction of Zr(IV). Surface coverage of ILs (SG-APTMS-N, N-EPANTf₂) was characterized by FT-IR and SEM. This process offered simplicity and effectiveness of the selective extraction materials for Zr(IV) in aqueous samples with acceptable precision.

As mentioned, there are researches which successfully prepared humic acids and ionic liquids immobilized onto solid sorbents, and also displayed potential to heavy metal ions removal which can be benefit for this work. Thus in this study, ionic liquids and humic acids immobilization onto aminopropyl silica were prepared and applied for the separation of Au and Ag ions/nanoparticles in aqueous solution and their concentration was measured by inductively coupled plasma-optical emission spectrometry (ICP-OES).

CHAPTER III
EXPERIMENTAL

3.1 Chemical

All chemicals used in this research are listed in Table 3.1.

Table 3.1 List of chemicals

Chemicals	Supplier
Silver standard solution (1000 mg/L)	Merck
Gold standard solution (1000 mg/L)	Merck
Silver nitrate, AgNO ₃	Merck
Sodium borohydride, NaBH ₄	Merck
Starch soluble GR for analysis	Merck
Tri-sodium citrate	Fisher Scientific
Hexadecyltrimethylammonium bromide	Merck
Hydrogen peroxide, H ₂ O ₂	Merck
Ethanol	Merck
Toluene	Carlo Erba
Chloroform	Merck
Acetone	Merck
Sodium hydroxide, NaOH	Merck
Hydrochloric acid 37%, HCl	Merck
Nitric acid 65%, HNO ₃	Merck
Sulfuric acid, H ₂ SO ₄	Merck
Thiourea	Sigma aldrich
Silica gel, 70-230 mesh	Merck
3-Aminopropyltriethoxysilane	Sigma Aldrich

Table 3.1 (cont.)

Chemicals	Supplier
Humic acids	Sigma aldrich
Chloroacetic acid	Sigma aldrich
1-Methylimidazole	Sigma aldrich

3.2 Instruments

The instruments employed in this research are shown in Table 3.2.

Table 3.2 List of instruments

Instruments	Model, Manufacturing company
Inductively coupled plasma-optical emission spectrometer (ICP-OES)	iCAP 6500 DUO, Thermo Scientific
pH meter	SevenCompact pH/Ion s220, METTLER TOLEDO
Overhead mixer	Rotax 6.8, VELP SCIENTIFICA
Vacuum pump	V-700, Buchi
Centrifuge	Universal 32 R, Hettich
Fourier transform infrared spectrometer (FT-IR)	Nicolet 6700, Thermo Scientific
Surface area analyzer	Autosorb-1, Quantachrome
Diffuse reflectance ultraviolet visible spectrometer (DR-UV-Vis)	UV-2500PC, Shimadzu
Ultraviolet visible spectrophotometer (UV-Vis)	Agilent 8453

The operation conditions in this research for the determination of silver and gold ions/nanoparticles by ICP-OES are shown in Table 3.3.

Table 3.3 ICP-OES conditions for the determination of silver and gold ions/nanoparticles

Conditions	Values
Gold emission wavelength	242.795 (nm)
Silver emission wavelength	328.068 (nm)
Radio frequency power	1150 (W)
Auxiliary gas flow	0.5 (L/min)
Nebulizer gas flow	0.5 (L/min)
Coolant gas flow	12 (L/min)
Flush pump rate	50 (rpm)
Plasma view	Axial
Repeatability	3 (replicates)

3.3 Preparation of gold nanoparticles (AuNPs)

In this study, a AuNPs solution was prepared by using Au(III) solution (10 mg L^{-1}).

3.3.1 Preparation of reducing reagent

A sodium borohydride (NaBH_4) solution (10 mM) for the reduction of Au(III) was prepared by dissolving in DI water. This solution was freshly prepared for each synthesis batch.

3.3.2 Preparation of stabilizer

Starch solution

Soluble starch for analysis (2 g) was slowly added to boiling DI water (100 mL) until the starch was dissolved. After completing the mixing, the starch solution was allowed to cool down at room temperature and incubated with diluted NaOH prior to use.

Tri-sodium citrate and hexadecyltrimethylammonium bromide (CTAB)

The solutions were prepared by dissolving tri-sodium citrate (0.37 g) and CTAB (0.46 g) in DI water (25 mL).

3.3.3 Preparation of AuNPs

The NaBH_4 solution was gently added into Au(III) solution. After the addition was complete, the solution appeared red in color of AuNPs by visual observation. The synthesized AuNPs was then gently mixed with stabilizer of tri-sodium citrate and CTAB. Meanwhile, the starch stabilized AuNPs was prepared by mixing boiled Au(III) solution at 100 °C and prepared starch solution (2% w/v) together under vigorous stirring [79]. After a few minutes, the final AuNPs solution became red in color and the solution was cooled down at room temperature prior to use. The absorption spectra of AuNPs were observed by UV-Vis in the wavelength range of 400-800 nm.

3.4 Preparation of silver nanoparticles (AgNPs)

3.4.1 Preparation of AgNPs using starch stabilizer

The preparation of AgNPs was adapted from silver nanospheres (AgNSs) method proposed by Wongravee et. al. [80]. AgNPs solution was prepared by using AgNO_3 (1.57 g) and NaBH_4 (0.52 g), each of them was dissolved in 500 mL of starch solution (2% w/v). The solution was mixed at a rate of 2 mL s^{-1} under vigorous stirring. The dark brown solution was obtained, illustrating a formation of AgNPs. The total volume of the solution was adjusted to 1300 mL with DI water and stirring continued for 30 minutes. The solution was boiled again at $100 \text{ }^\circ\text{C}$ for 2 hours and then cooled down at room temperature as well as aged for 12 hours. The final volume of AgNPs solution was adjusted to 1000 mL with DI water in order to obtain the total silver content of 1000 mg L^{-1} .

3.4.2 Preparation of AgNPs using citrate stabilizer

AgNPs solution synthesized by using tri-sodium citrate was adapted from Kaur et. al. [81]. The AgNPs solution was prepared by using a precursor of AgNO_3 (0.016 g) and tri-sodium citrate (0.029 g) as a reducing agent. The solution of AgNO_3 (100 mL) was boiled at $100 \text{ }^\circ\text{C}$ and tri-sodium citrate was added dropwise to the solution under vigorous stirring until the dark yellow solution was obtained. The solution was kept at room temperature with the total silver content of 100 mg L^{-1} .

3.5 Preparation of aminopropyl silica (SiAP)

Silica gel (50 g) was refluxed with dried toluene (200 mL) under nitrogen atmosphere for 2 hours at $150 \text{ }^\circ\text{C}$. Then 3-aminopropyltriethoxysilane (20 mL) was added dropwise [74] and the mixture was further refluxed for 24 hours. The SiAP solid was collected after filtered and washed with ethanol, and dried at $100 \text{ }^\circ\text{C}$ for 24 hours. The SiAP solid was characterized by FT-IR and a surface area analyzer.

3.6 Synthesis of 1-carboxymethyl-3-methylimidazolium chloride ionic liquid, [MimCM]Cl

[MimCM]Cl was synthesized by dissolving chloroacetic acid (9.45 g) in chloroform (80 mL) at room temperature. Then 1-methylimidazole (7.97 mL) was added dropwise to a solution and refluxed at 70 °C for 50 hours under nitrogen atmosphere. [MimCM]Cl solid was filtered and washed with ethanol for several times prior to dry at 60 °C for 24 hours [82].

3.7 Immobilization of [MimCM]Cl onto SiAP

The preparation of [MimCM]Cl-modified SiAP was adapted from Pu et. al. [77]. SiAP (11 g) and [MimCM]Cl (7 g) was added to acetone until slurry mixture was obtained and the mixture was heated at 140 °C for 30 minutes. The final product was kept in a desiccator prior to characterize by FT-IR and a surface area analyzer.

3.8 Immobilization of HA onto SiAP

HA (1.2 g) was prepared in 60 mL of solution containing 0.1 M NaOH and then SiAP solid (2 g) was added in the solution. The final volume of the mixture was adjusted to 100 mL with DI water and adjusted to pH range of 7.5-8.0. The mixture was stirred for 20 hours at room temperature. The SiAP-HA solid was separated from the mixture by centrifugation. The solid was filtered, washed several times with DI water, and dried at 120 °C for 5 hours. After curing, the solid was washed again with a solution of pH 10 to eliminate the loosely bound HA [74]. The SiAP-HA was characterized by FT-IR, surface area analyzer, and DR-UV-Vis.

3.9 Optimization of Au and Ag ions/nanoparticles extraction

3.9.1 Effect of pH

The effect of pH on the extraction behavior of Au and Ag ions/nanoparticles was firstly investigated. The pH of solutions was adjusted to pH range of 2-10 with diluted HNO_3 and NaOH . In this experiment, SiAP-ILs and SiAP-HA adsorbents (0.05 g of each) were used for the extraction procedure of Au ions/nanoparticles and Ag ions/nanoparticles, respectively. Moreover, SiAP sorbent was employed to monitor the extraction efficiency of metals in comparison to the modified-adsorbents. The mixture of 10 mL of metal solution (10 mg L^{-1}) and adsorbent was shaken at room temperature for 60 minutes to ensure the adsorption equilibrium. Finally, the supernatant was separated by centrifugation at 3000 rpm for 5 minutes and filtered through a $0.45 \mu\text{m}$ membrane. The residual of metal concentration in supernatant was analyzed by ICP-OES and the extraction efficiency percentage (%EE) was reported.

3.9.2 Effect of time

In this experiment, the extraction of Au and Ag ions/nanoparticles as a function of time was studied in the range of 5-60 minutes. The extraction time was investigated at a fixed optimal pH range with 0.05 g of adsorbents with the concentration of 10 mg L^{-1} of metal solutions (10 mL). The mixture was shaken at room temperature for various times (5-300 minutes for Au/AuNPs and 5-60 minutes for Ag/AgNPs) and then the supernatant was separated by centrifugation prior to filter through a $0.45 \mu\text{m}$ membrane. The residual metal concentration in supernatant was determined by ICP-OES and reported as the extraction efficiency percentage (%EE).

3.9.3 Adsorption isotherm

A suspension of 0.05 g of adsorbent in 10 mL of metal solution was equilibrated using varied concentration range between 10-300 mg L⁻¹ under optimum pH range in a test tube. The mixture was stirred at room temperature and optimum extraction time and the temperature was controlled at 298 ± 1 K. The solid sorbent was separated by centrifugation at 3000 rpm for 5 minutes. Residual metal concentration of the supernatant was determined by ICP-OES after 0.45 µm membrane filtration.

3.10 Separation of metal ions/nanoparticles

In the separation process, 10 mL of Au and Ag ions/nanoparticles (5 mg L⁻¹ of each) was added into a test tube containing 0.05 g of adsorbents. The mixture solution was adjusted to a desired pH range with diluted HNO₃ and NaOH. The mixture was then shaken at room temperature at optimum extraction time. The resulting metal loaded on SiAP-ILs and SiAP-HA was isolated using centrifugation and then the supernatant containing M-NPs was filtered through a 0.45 µm membrane. The residual of M-NPs concentration in supernatant was determined by ICP-OES and the recovery percentage (%recovery) was reported. Meanwhile, the solid sorbents were kept for further elution process.

3.11 Elution procedure

Several eluents were used for the desorption study of metal ions from adsorbent. In this experiment, 0.1 M of HNO₃, H₂SO₄, and thiourea were chosen. For this proposed method, the adsorbent was taken into 10 mL of each eluent and the mixture was shaken for 15 minutes. Finally, the mixture was isolated through a 0.45 µm membrane filter prior to analyze by ICP-OES and the concentration of metal ions in term of recovery percentage (%recovery) was calculated.

3.12 Sequential elution procedure

The sequential elution process was studied for the separation of Ag(I) ions and AgNPs from SiAP sorbent. Several eluents (0.1 M of HNO₃, H₂SO₄, and thiourea) were used for the desorption of Ag(I) ions and AgNPs from SiAP sorbent. For this propose method, 10 mL of 5 mg L⁻¹ Ag(I) and AgNPs solution were prepared and the extraction process was performed as mentioned above. The adsorbent was isolated by using centrifugation, then it was taken into the eluent and the mixture was shaken for 15 minutes. The mixture was centrifuged again to separate a metal solution from the adsorbent and a solution was filtered through 0.45 µm membrane filter prior to analyze by ICP-OES. Then the remaining adsorbate was re-dispersed again in 10 mL of eluent for 15 minutes after oxidized with 2 (%v/v) H₂O₂. Afterward, the solution was filtered through 0.45 µm membrane filter and analyzed by ICP-OES.

3.13 Method validation

Validation of analytical method is the measurement of performance characteristics such as accuracy, precision, limit of detection (LOD), limit of quantitation (LOQ), linearity, and range. In this proposed method, the determination of Au and Ag ions/nanoparticles was quantified and reported in the term of accuracy and precision. And this method was validated by using spiked real samples with Au and Ag ions/nanoparticles solution.

Real samples employed in this work were collected from jewelry wastewater of the Gem and Jewelry Institute of Thailand, underground water from Khamphaeng Phet province, and the effluent from Thawi watthana district of Bangkok. These three samples were utilized for the determination of Au ions and nanoparticles. The household products of the Nano seven pets (odor removal spray) and the Nanosilver product of Chulalongkorn University (for get rid of bacteria) were used for the determination of Ag ions and nanoparticles.

3.13.1 Accuracy and precision

Initially, real samples were analyzed by ICP-OES in order to obtain the total metal contents. The adsorbent of SiAP-ILs and SiAP-HA (0.05 g of each) was used for the isolation of Au ions/nanoparticles and Ag ions/nanoparticles, respectively, containing in real samples which adjusted to optimal pH range. The proposed method was performed by employing spiked real samples with Au and Ag ions/nanoparticles solution at a concentration of 1 mg L^{-1} . Each experiment was repeated 3 times. The binary mixtures of metal ions and nanoparticles in real samples were shaken at optimum extraction time and then separated by centrifugation and the supernatant was filtered through a $0.45 \text{ }\mu\text{m}$ membrane prior to analyze by ICP-OES. The solid sorbents were taken into the optimal eluent (10 mL) and further shaken for 15 minutes. Afterward, the solution was filtered through a $0.45 \text{ }\mu\text{m}$ membrane and analyzed by ICP-OES. The accuracy and precision of the proposed method were calculated and illustrated in the term of recovery percentage (%recovery) and relative standard deviation percentage (%RSD).

3.13.2 Limit of detection (LOD)

Blank solution of DI water was analyzed. The signal of Au and Ag at emission wavelength of 242.795 nm and 328.068, respectively, was observed by ICP-OES in 10 replicates. The LOD was calculated from the mean of blank signal and 3 times of standard deviation (SD).

CHAPTER IV

RESULTS AND DISCUSSION

4.1 Characterization of SiAP-IL

The SiAP-IL solid sorbent was synthesized via 1-carboxymethyl-3-methylimidazolium chloride ionic liquid [MimCM]Cl immobilized onto aminopropyl silica sorbent which showed schematically in Figure 4.1. The synthesized SiAP-IL was characterized by FT-IR and surface area analysis compared with SiAP and [MimCM]Cl ionic liquids.

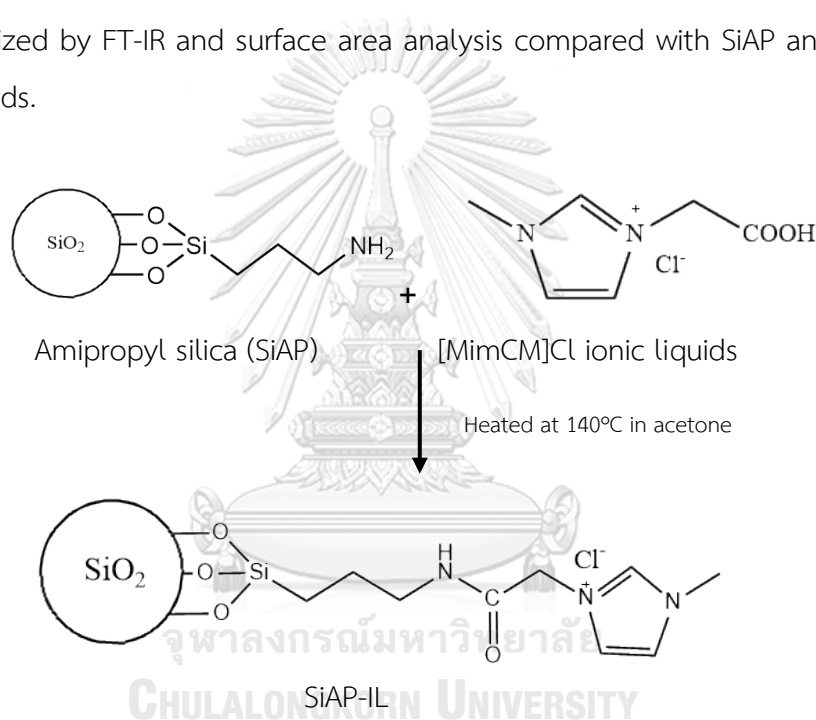


Figure 4.1 Schematic representation of the immobilization between SiAP and [MimCM]Cl.

4.1.1 Fourier transform infrared spectroscopy (FT-IR)

The FT-IR spectra of aminopropyl silica (SiAP), [MimCM]Cl ionic liquids and [MimCM]Cl ionic liquids modified-aminopropyl silica (SiAP-IL) in the wavenumber range of 500-4000 cm^{-1} are illustrated in Figure 4.2. The characteristic peak of SiAP is at 1100 cm^{-1} which corresponds to Si-O-Si stretching as well as N-H stretching of

amino group at 3460 cm^{-1} . For [MimCM]Cl ionic liquids, the peaks at 1643 and 1738 cm^{-1} are assigned to N-H bending and C=O stretching. The stretching vibration peak of the C-N bond appears at around $1250\text{--}1350\text{ cm}^{-1}$. For the modified silica with [MimCM]Cl, the presence of the characteristic peaks at 1735 and 1635 cm^{-1} , arising from amide bond (-NHC=O) which is an evidence of the chemical reaction between SiAP and [MimCM]Cl ionic liquids. This result showed that [MimCM]Cl ionic liquids was successfully immobilized onto SiAP.

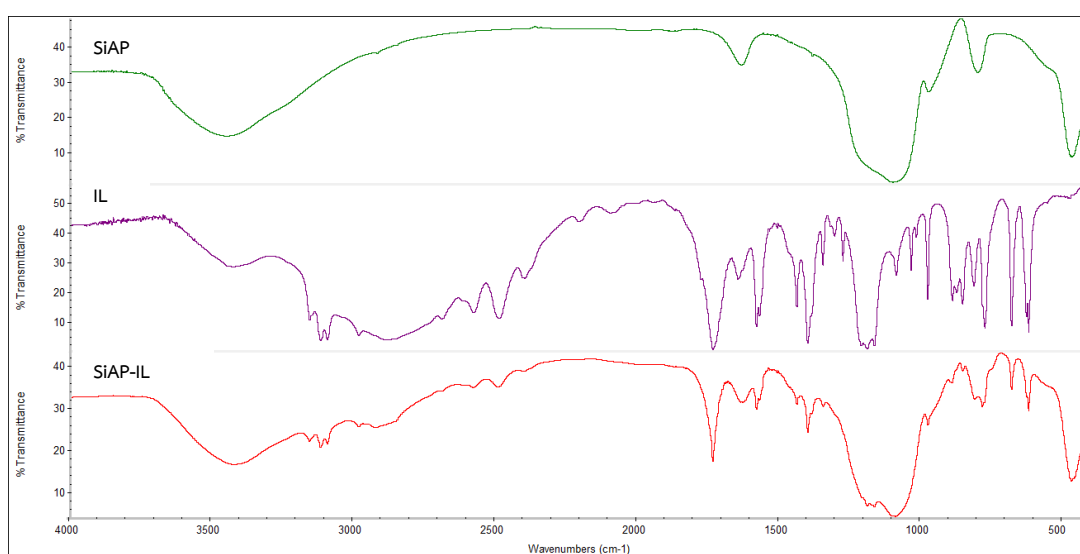


Figure 4.2 FT-IR spectra of aminopropyl silica (SiAP), [MimCM]Cl ionic liquid and [MimCM]Cl ionic liquid modified-aminopropyl silica (SiAP-IL).

4.1.2 Surface area analysis

The surface area and pore volume of adsorbents were investigated by using BET surface area analysis (Table 4.1).

Table 4.1 Summary of the adsorbent parameters measured by surface area analysis

Adsorbent	BET surface area ($\text{m}^2 \text{g}^{-1}$)	Total pore volume ($\text{cm}^3 \text{g}^{-1}$)
SiAP	284.88	0.4075
SiAP-IL	99.67	0.2057

The results in Table 4.1 show that surface area and pore volume of modified-SiAP was obviously decreased when compared to SiAP. Thus, all data above supported that the functionalized [MimCM]Cl ionic liquids was completely immobilized onto the surface and the SiAP pore.

4.2 Gold nanoparticles

As for nanoparticles size is depend on surrounding medium, the plasmon resonance (SPR) of MNPs can be observed via spectrophotometric method. For instance, if the size of nanoparticle changes, the transformation of surface geometry also occurs which leads to a shift in the electric field density on the surface and changing the oscillation frequency of the electrons. In this work, the unique optical property of gold nanoparticles (SPR) was observed via UV-Vis spectrometry. Tri-sodium citrate, CTAB and starch were used as a stabilizer in order to prevent aggregation of AuNPs. After addition of the reducing agent and stabilizers, the color of AuNPs (10 mg L^{-1}) solution became pale red. On the other hand, the color of AuNPs without stabilizer changed to purple rapidly after addition of the reducing agent.

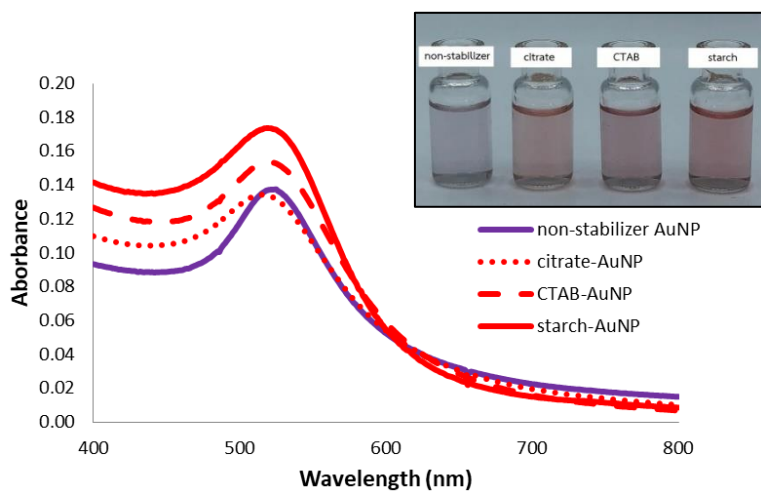


Figure 4.3 Visible spectrum of gold nanoparticles.

The result of the SPR absorption band of AuNPs with different stabilizers and non-stabilizer was shown in Figure 4.3. It has spectroscopically distinct red phase which showed the maximum absorption around wavelength of 517-519 nm for AuNPs with stabilizers. Meanwhile, the purple phase of AuNPs without stabilizer showed the maximum absorption around 525 nm. According to the finding of Link et. al., the size dependence of the plasmon absorption was investigated in aqueous solution and displayed extinction spectra of AuNP of various sizes in Figure 4.4. It was clearly that if the SPR band in visible region shift to longer wavelength, the particle size was increase [83].

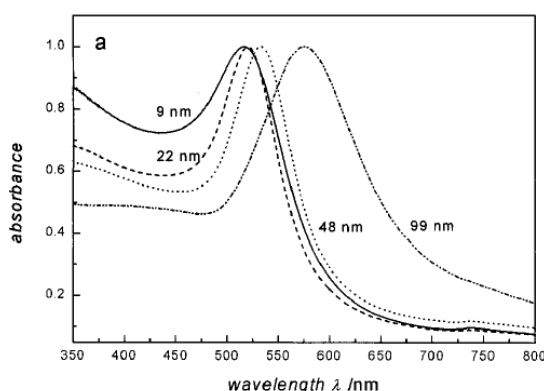


Figure 4.4 UV-Vis spectrum of AuNPs in aqueous solution with different diameter size [83].

Moreover, AuNPs with different stabilizers were characterized by TEM technique. TEM images of AuNPs are shown in Figure 4.5, illustrating spherical shape of the particles. This result showed that the aggregated AuNPs was clearly observed for AuNPs without stabilizer in Figure 4.5 (a) with varied particle sizes. Meanwhile, tri-sodium citrate and starch could be implied as a good stabilizer to prevent the aggregation of AuNPs as showed in Figure 4.5 (b) and (c). In this experiment, the estimation diameter size of AuNPs with stabilizer was around 9-15 nm. Whereas AuNPs without stabilizer was tending to larger particles (>20 nm) which corresponds to purple color of the solution due to an aggregation. This average diameter size of AuNPs was similar to the finding of Link et al. [Ref.]. The image of CTAB-stabilized AuNPs was unable to record due to a burning of CTAB under electron beam.

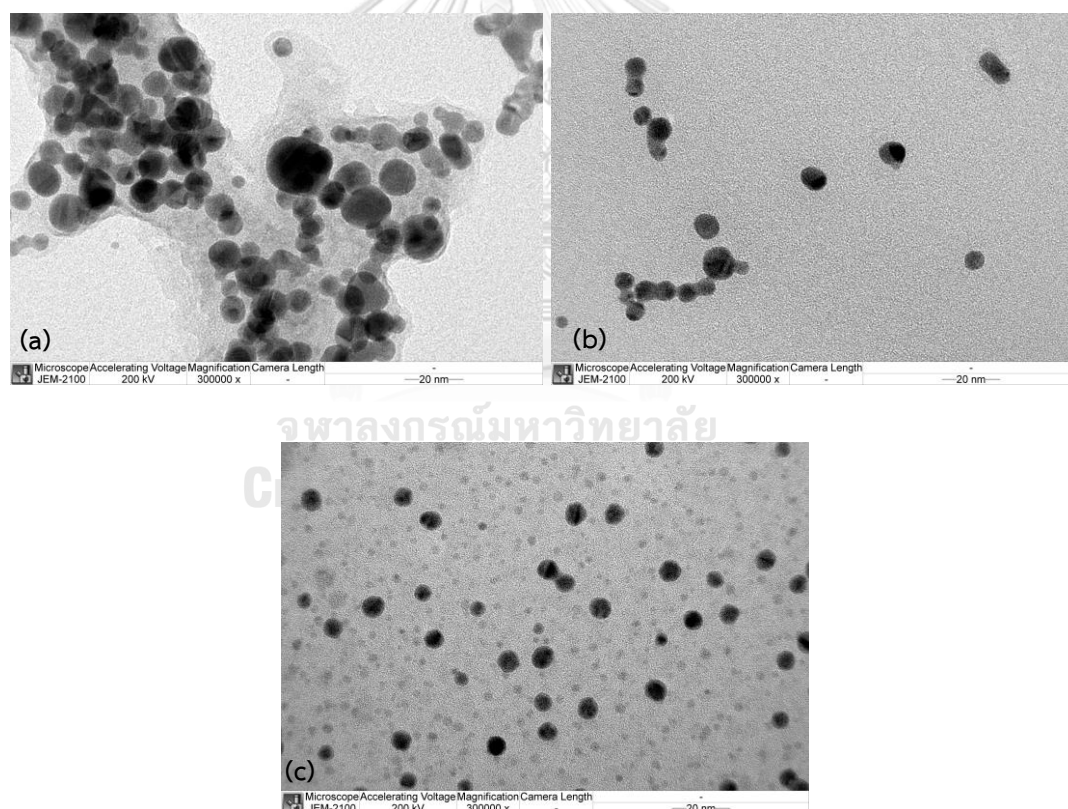


Figure 4.5 TEM images (300,000 × magnification) of (a) non-stabilizer AuNPs (b) citrate-AuNPs and (c) starch-AuNPs.

4.3 Optimization of Au ions/nanoparticles extraction

4.3.1 Effect of pH

The pH plays significant roles in the adsorption process of metals onto solid sorbent surfaces. In this experiment, the pH values on the extraction of Au(III) ions and Au nanoparticles were adjusted to 2-7. The extraction time was fixed at 60 minutes to ensure the adsorption equilibrium and the results are shown in Figure 4.6.

The extraction efficiency of Au(III) and AuNPs was reported in term of extraction efficiency percentage (%EE), according to equation 4.1

$$\%EE = \left(\frac{C_i - C_f}{C_i} \right) \times 100 \quad (4.1)$$

Where C_i = the initial concentration of metal (mg L^{-1})
 C_f = the final concentration of metal in supernatant (mg L^{-1})

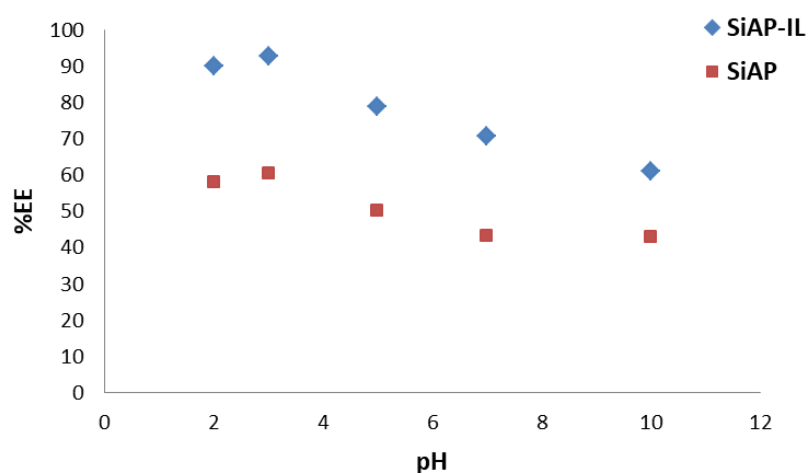


Figure 4.6 Effect of pH on the extraction of Au(III) by SiAP and SiAP-IL.

The result showed that the extraction efficiency of Au(III) for both adsorbents increased and followed by a subsequent decrease with an increase of pH range. It was probably due to the prevention by hydrogen cations in acidic medium for dissociation of HAuCl_4 at pH 2, decreasing extraction efficiency of Au(III). While at pH 3, the formation of AuCl_4^- occurred and showed quantitatively extracted into SiAP-IL sorbent. However, the extraction efficiency was rapidly decreased with further increased of pH from 5 to 10. This phenomena was probably due to the possible formation of Au(III) with hydroxide ions to form complex of $[\text{AuCl}_3(\text{OH})]^-$ which previously reported [84]. Therefore, the potential of AuCl_4^- binding with SiAP-IL surface was decreased. Thus, pH 3 was chosen for further studies.

Since SiAP-IL displayed higher efficiency for extraction of Au(III), it was selected for additional study of AuNPs. In this study, different types of AuNPs stabilizer were used to observe their influence on the extraction efficiency by the adsorbent such as tri-sodium citrate, CTAB, starch and non-stabilizer as well. The extraction time was fixed at 60 minutes according to recently process.

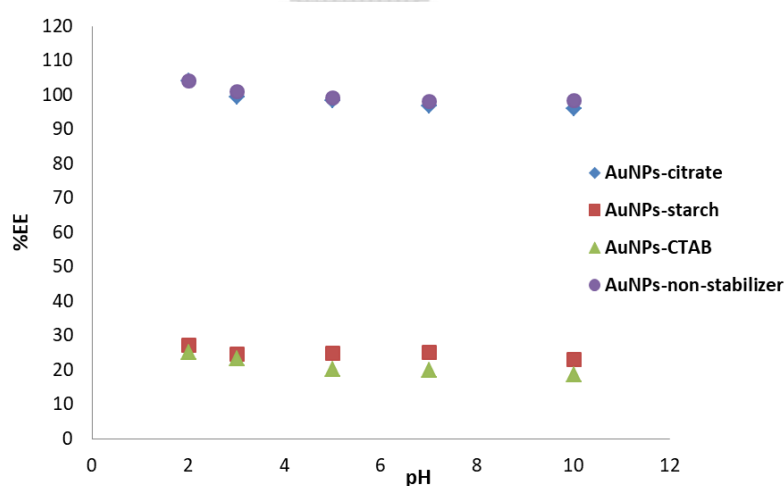


Figure 4.7 Effect of pH on the extraction of AuNPs by SiAP-IL.

The extraction efficiency of AuNPs using SiAP-IL at various pH ranges are shown in Figure 4.7. The results showed that AuNPs prepared by tri-sodium citrate and non-stabilizer displayed higher extraction efficiency over 90% in all pH range. Consistency with the color of both solutions appeared purple after adjusting

pH less than 3 due to the aggregation of AuNPs. Meanwhile, the pale red color of AuNPs did not change when their pH value remained in the range of 3-10. However, the purple color of non-stabilizer AuNPs and citrate-stabilized AuNPs were observed on the SiAP-IL surface after extraction time of 60 minutes as well as colorless of supernatant was observed. Theoretically, a stable surface charge of citrate stabilized-AuNPs in Figure 4.8 (a) showed negatively charge of carboxylate groups which provided repulsion force and prevented them to aggregate [85]. Therefore, the aggregation was occurred in acidic medium of pH 2 due to the protonation of hydrogen ions which reduced the repulsion force of nanoparticles. In addition, the negative charge of AuNPs surface was probably assembled onto SiAP-IL surface which was observed for higher extraction efficiency. Meanwhile, non-stabilizer AuNPs revealed rapidly aggregation in all pH range and shortly precipitated onto adsorbent surface.

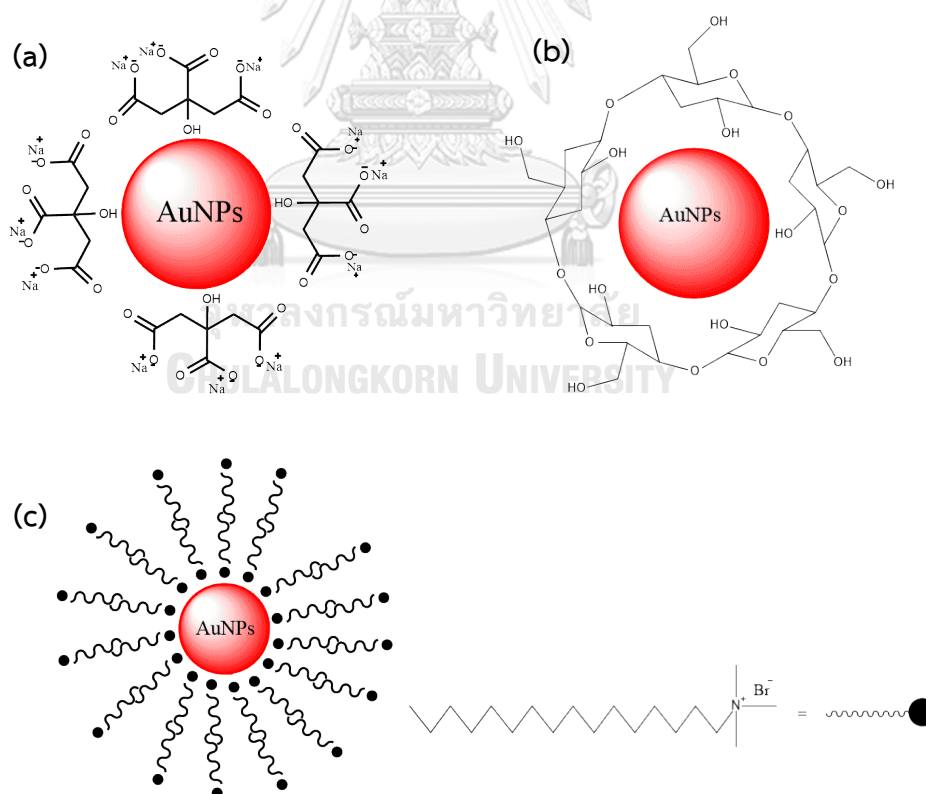


Figure 4.8 Schematic representations of various types of stabilizer immobilized-AuNPs (a) tri-sodium citrate (b) starch and (c) CTAB.

Notably, CTAB and starch stabilized AuNPs showed lower extraction efficiency through SiAP-IL sorbent in all pH range. The schematic representation of starch and CTAB stabilized AuNPs are shown in Figure 4.8 (b) and (c), respectively. In this study, starch stabilized AuNPs was synthesized without further surface modification [79]. As for the formation of starch stabilized AuNPs mainly contained hydroxyl-rich, highly dispersion of nanoparticles was observed [86]. Moreover, the pKa of starch hydroxyl group was reported around 12.6 which likely dissociated at higher pH value [87]. The hydroxyl group on starch surface was not dissociated at lower pH range and therefore they were not adsorbed on the sorbent surface at the pH range of this observation. According to the study finding, starch stabilized AuNPs exhibited a little adsorption behavior onto adsorbent within 60 minutes and remained pale-red color of AuNPs in supernatant. Meanwhile, the hydrophobic bilayer of CTAB was presented on AuNPs surface [88] and thereby a high positively charged surface occurred [89] which is not suitable for binding with adsorbent surface. This might be a reason for lower extraction efficiency of CTAB stabilized AuNPs using SiAP-IL.

4.3.2 Effect of time

The effect of extraction time on the extraction efficiency of Au(III) ions and Au nanoparticles were studied by using the optimal pH of 3 from previous experiment. The results of extraction efficiency of Au(III) ions using unmodified-SiAP compared with SiAP-IL ions are shown in Figure 4.9. The results demonstrated that Au(III) was favorable adsorbed onto SiAP-IL rather than SiAP. Moreover, the extraction efficiency of Au(III) ions onto SiAP-IL was increased greater than 90% in all ranging time of 5 to 300 minutes and reached an equilibrium within 30 minutes.

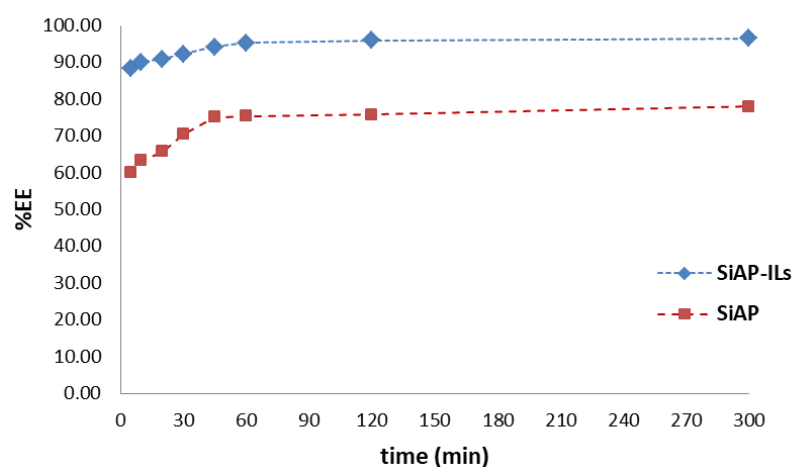
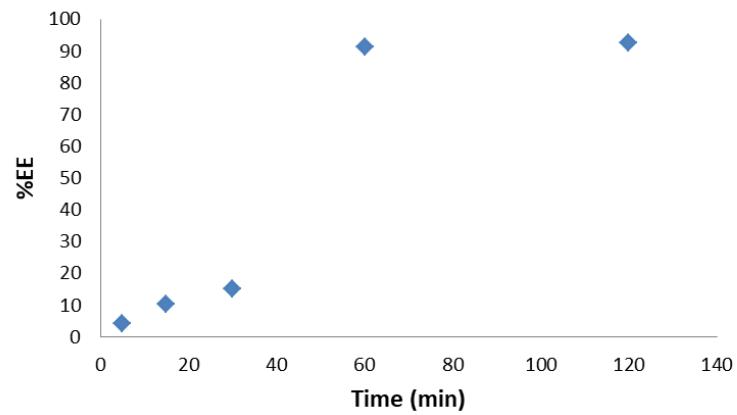
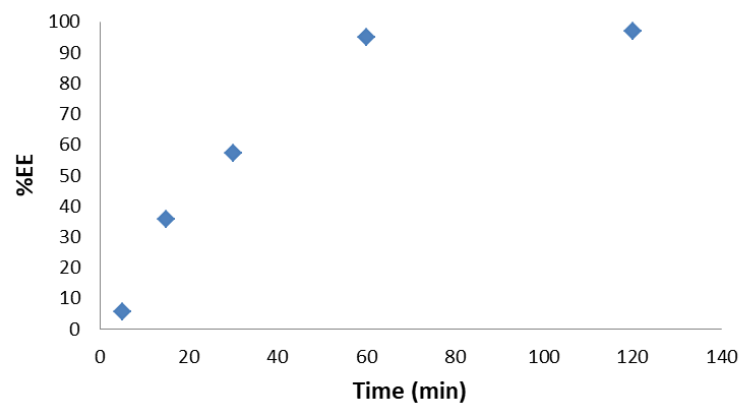
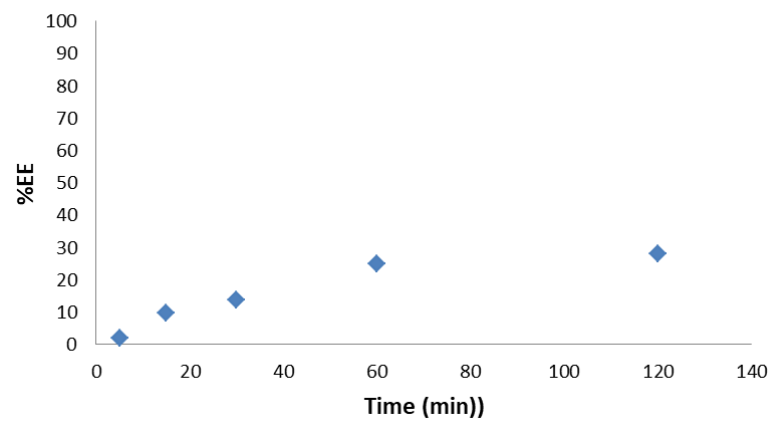


Figure 4.9 Effect of extraction time on the extraction of Au(III) using SiAP-IL.

Gold nanoparticles were further investigated extraction time affecting the extraction efficiency using SiAP-IL adsorbent (Figure 4.10). It was found that non-stabilizer and citrate stabilized AuNPs showed higher extraction efficiency after 30 minutes as results of color change from pale-red to colorless in the supernatant. It was likely attributed to an effect of anionic stabilizer which can be displayed a high affinity to adsorbent surface, while non-stabilizer was easily aggregated and precipitated onto the adsorbent surface. On the other hand, the low extraction efficiency was obtained for starch and CTAB stabilized AuNPs. The possible explanation for these results depends on an inappropriate surface charge between AuNPs stabilizer and adsorbent surface as discussed in previous study. However, the lowest extraction efficiency was observed within 5 minutes and used as optimum extraction time for further studies.

Extraction efficiency of AuNP (non-stabilizer)**Extraction efficiency of AuNPs (tri-sodium citrate)****Extraction efficiency of AuNPs (starch)**

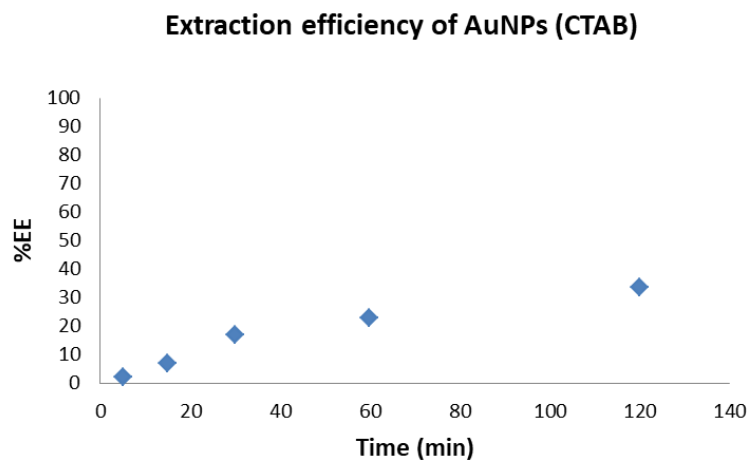


Figure 4.10 Effect of extraction time on the extraction of AuNPs using SiAP-IL.

4.4 Adsorption isotherm of Au(III)

The equilibrium conditions of adsorption process were studied using Langmuir and Freundlich models. The Langmuir isotherm represents maximum adsorption to the saturated monolayer adsorption onto the sorbent surface [90]. The equation is:

$$\frac{C_e}{q_e} = \frac{C_e}{q_m} + \frac{1}{K_L q_m} \quad (4)$$

Where

- q_e = the amount of metal ions adsorbed on the adsorbent (mg g^{-1})
- C_e = the equilibrium metal ion concentrations in the solution (mg L^{-1})
- K_L = the Langmuir isotherm constant (L mg^{-1})
- q_m = the maximum amount of metal ions adsorbed per gram of the adsorbent (mg g^{-1})

The Freundlich isotherm is generally used to describe multilayer adsorption [90] and the equation can be expressed as follows:

$$\log q_e = \log K_f + \left(\frac{1}{n} \right) \log C_e \quad (4.3)$$

Where q_e = the amount of metal ions adsorbed on the adsorbent (mg g^{-1})
 C_e = the equilibrium metal ion concentrations in the solution (mg L^{-1})
 n = the Freundlich constant
 K_f = the Freundlich constant (L g^{-1})

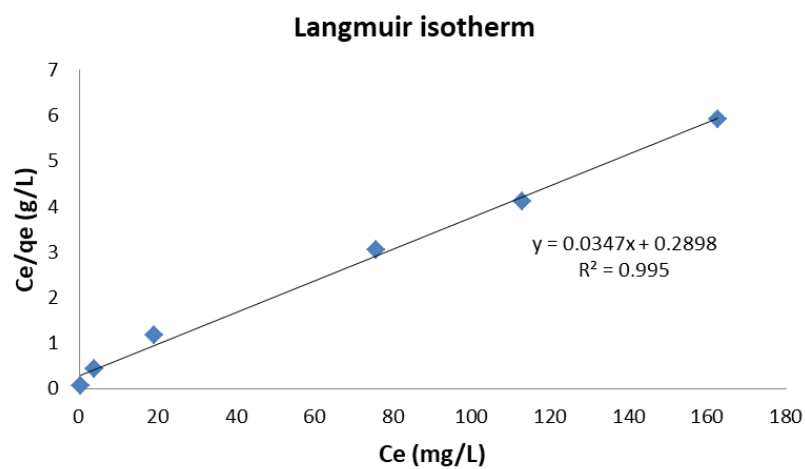


Figure 4.11 Langmuir isotherm of Au(III) onto SiAP-IL.

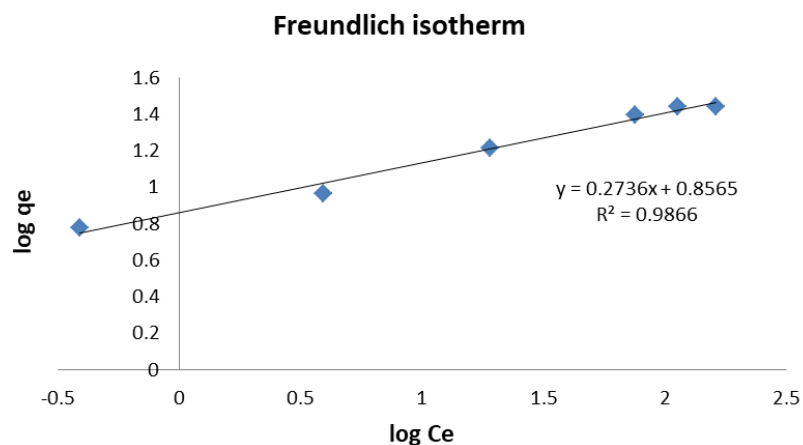


Figure 4.12 Freundlich isotherm of Au(III) onto SiAP-IL.

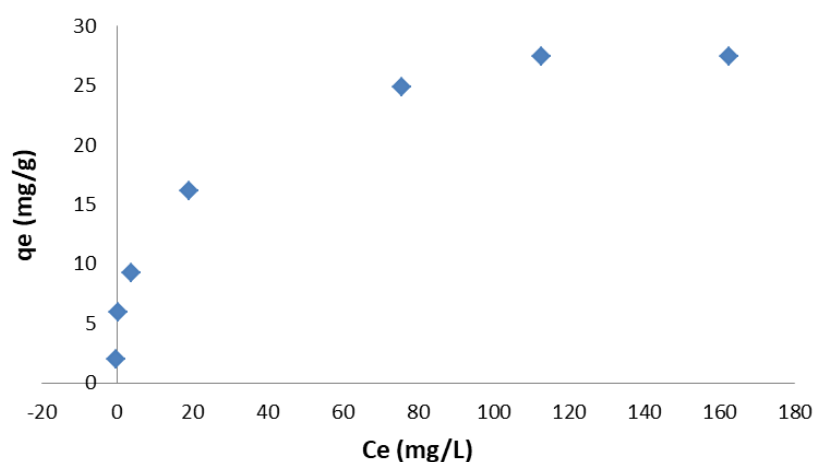


Figure 4.13 Adsorption isotherm of Au(III) onto SiAP-IL.

This result could be explained for Au(III) ions because AuNPs displayed low adsorption by SiAP-IL. A comparison of Langmuir and Freundlich models was investigated for the adsorption behavior of Au(III) by SiAP-IL at pH 3 and 298 K. The adsorption isotherm experiments were studied by varying initial concentration of Au(III) in the range of 10 to 300 mg L⁻¹ and stirring time was 5 minutes. The Langmuir model is represented a monolayer sorption onto the homogeneous surface with specific number of equivalent sites, according to equation 4.2. Whereas, the Freundlich model is defined as multilayer sorption related to equation 4.3.

The adsorption data in Figure 4.11 reveal that the Langmuir model showed the best correlation with the experimental data which indicated that the adsorption of Au(III) ions on SiAP-IL surface was monolayer with a maximum capacity of 28.25 mg g⁻¹. The calculated parameters of K_L and R^2 are 0.12 L mg⁻¹ and 0.995, respectively. Furthermore, the adsorption isotherm behavior of Au(III) onto SiAP-IL in Figure 4.13 showed that Au(III) ions adsorbed on the adsorbent was reached a plateau at around 28 mg g⁻¹ consistent with a maximum capacity value from the Langmuir model.

4.5 Separation of Au ions/nanoparticles

A binary mixture of Au(III) and AuNPs was investigated by using SiAP-IL sorbent. The separation of metal species can be observed after a mixture of metal solution was subjected to sorbent. For this proposed method, AuNPs was not suitable for binding with sorbent and remained in the solution, while Au(III) ions in the formation of AuCl₄⁻ was preferable adsorbed onto SiAP-IL surface.

In this experiment, a binary solution of Au(III) and AuNPs (5 mg L⁻¹ of each) at pH 3 was subjected to SiAP-IL sorbent for 5 minutes. After complete extraction, the color of solution sustained in pale red indicating that AuNPs remained in the solution and was not adsorbed onto SiAP-IL. However, SiAP-IL could be changed to red after extraction time over 30 minutes. The recovery of AuNPs in mixture solution by SiAP-IL was determined using ICP-OES and reported as recovery percentage (%recovery) which was defined in equation 4.4.

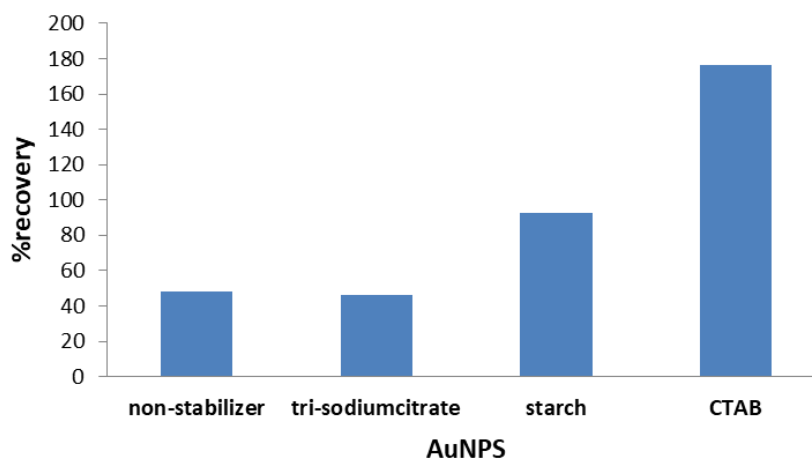


Figure 4.14 The recovery of AuNPs by SiAP-IL.

The recovery of AuNPs in Figure 4.14 illustrated that lower recovery percentage was observed when non-stabilizer and citrate stabilized AuNPs were subjected to adsorbent. Whereas, starch stabilized AuNPs obviously showed greater recovery more than 92%. However, the higher recovery over 100% was observed for CTAB stabilized AuNPs which probably due to positive surface charge of CTAB could be bound with Au(III).

The recovery percentage (%recovery) was defined in equation 4.4.

$$\%recovery = \frac{C_f}{C_i} \times 100 \quad (4.4)$$

Where C_f = the concentration of MNPs found in supernatant (mg L^{-1})
 C_i = the initial concentration of MNPs (mg L^{-1})

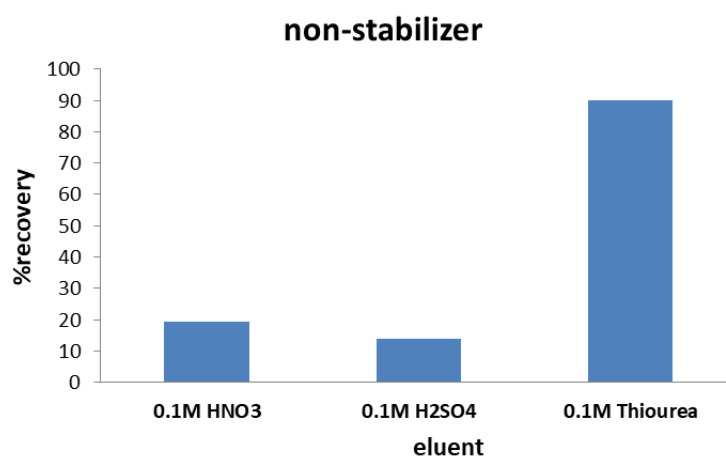
To determine Au(III) ions adsorbed onto SiAP-IL, the optimal eluent for adsorbed metal was further studied. The selectivity of eluent for Au(III) was investigated using various types of eluents and results are shown in Figure 4.15. The result showed that thiourea can quantitatively desorb Au(III) ions with high

efficiency (>90%), while lower elution efficiency was obtained when using HNO₃ and H₂SO₄. The higher elution efficiency of thiourea was probably due to the fact that thiourea can form a stable complex with Au(III) [91, 92], therefore Au(III) could be favorably desorbed from the adsorbent. Interestingly, the lowest elution efficiency of thiourea was examined for CTAB stabilized AuNPs. This might be a reason from previous study that Au(III) was already trapped with cationic of CTAB surfactant. The recovery of Au(III) was determined using ICP-OES and reported as recovery percentage (%recovery) which was defined in equation 4.5.

The recovery percentage (%recovery) was defined in equation 4.5.

$$\%recovery = \frac{C_e}{C_i} \times 100 \quad (4.5)$$

Where C_e = the concentration of metal eluted (mg L⁻¹)
 C_i = the initial concentration of metal (mg L⁻¹)



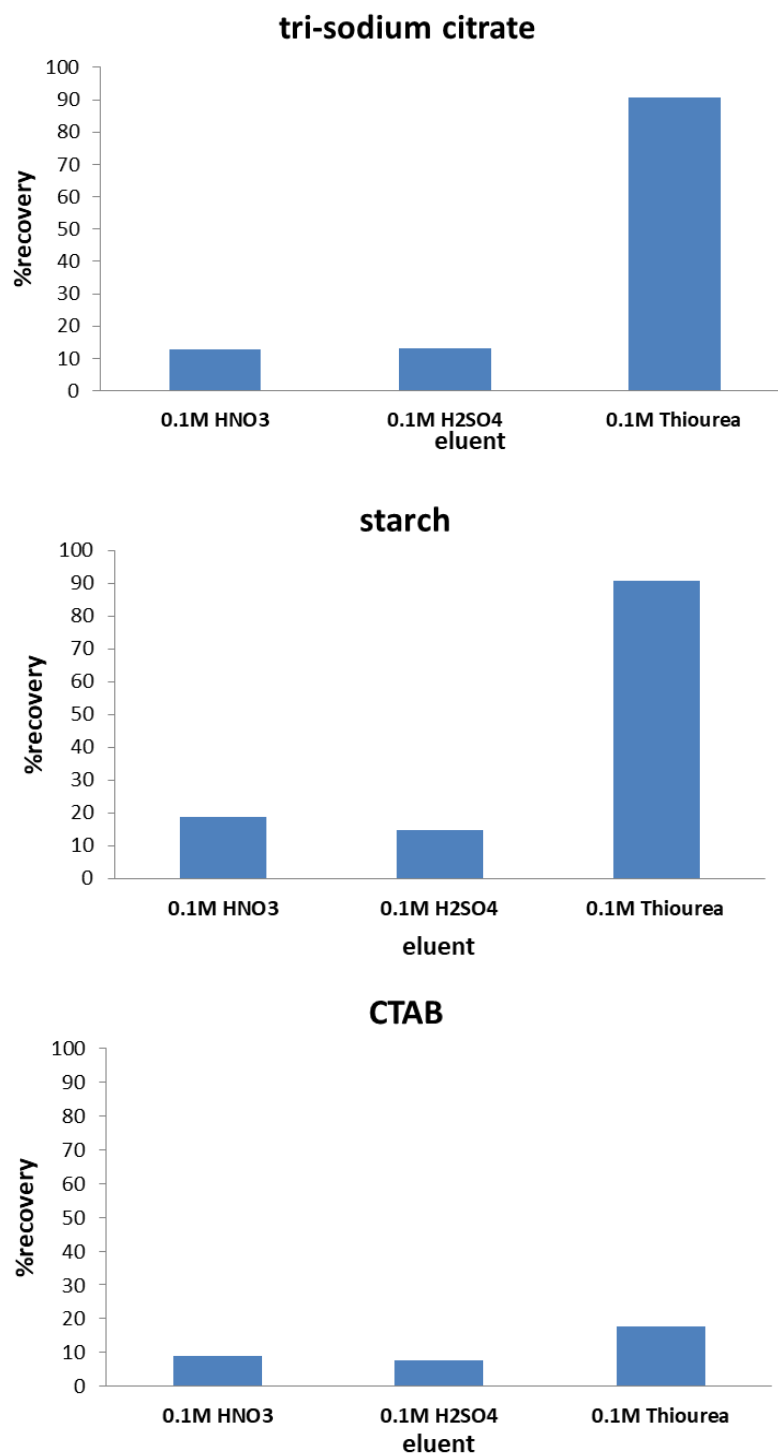


Figure 4.15 Elution of Au(III) ions using 0.1M HNO₃, 0.1M H₂SO₄ and 0.1M thiourea as eluents.

4.6 Method validation

The feasibility of the proposed method was evaluated by applying the optimal procedure to real samples. In this method, the determination of Au(III) and AuNPs in samples were quantified and reported in term of accuracy and precision. Moreover, the detection limit (LOD) was also evaluated.

The accuracy used for the measurement of the exactness of an analytical method or the closeness of agreement between the measured value and the true value. Whereas, the precision used for evaluate repeatability and reproducibility of measurements. The accuracy and precision was defined in equations 4.6 and 4.7.

$$\% \text{recovery} = \left(\frac{C_e - C_f}{C_i} \right) \times 100 \quad (4.6)$$

Where

- C_e = the concentration of metal eluted (mg L^{-1})
- C_f = the concentration of metal in unspiked sample (mg L^{-1})
- C_i = the initial concentration of metal spiked in sample (mg L^{-1})

$$\% \text{RSD} = \frac{\text{SD}}{\bar{X}} \times 100 \quad (4.7)$$

Where

- SD = the standard deviation
- \bar{X} = the mean value of metal concentration (mg L^{-1})

The detection limit (LOD) was evaluated using equation 4.8 which obtained from the mean and standard deviation of signals of ten replicates measurement of blank solution and compared with a standard calibration curve.

$$\text{LOD} = \bar{X}_{\text{blank}} + 3\text{SD}_{\text{blank}} \quad (4.8)$$

Where \bar{X} = the mean value of blank solution signal (mg L^{-1})

SD = the standard deviation of blank solution signal

Table 4.2 Analytical result of Au(III) ions and AuNPs in sample (n=3)

Samples	Ag species	Added (mg L^{-1})	Found (mg L^{-1})	Recovery (%)	RSD (%)
jewelry	Au(III)	0	2.77 ± 0.00	-	-
		1	3.65 ± 0.01	88.08	0.41
wastewater	AuNPs	0	1.01 ± 0.00^a	-	-
	(non-stabilizer)	1	1.02 ± 0.02	0.55	1.97
	Au(III)	0	2.77 ± 0.00	-	-
		1	3.66 ± 0.01	88.79	0.55
	AuNPs	0	1.01 ± 0.00^a	-	-
	(citrate)	1	1.27 ± 0.03	25.78	2.36
	Au(III)	0	2.77 ± 0.00	-	-
		1	3.68 ± 0.01	90.95	0.33
	AuNPs	0	1.01 ± 0.00^a	-	-
	(starch)	1	1.88 ± 0.01	86.40	0.53
	Au(III)	0	2.77 ± 0.00	-	-
		1	0.75	0	-
	AuNPs	0	1.01 ± 0.00^a	-	-
	(CTAB)	1	1.94 ± 0.03	92.87	1.55

^a The concentration found is estimated from remaining AuNPs in supernatant after separated with SiAP-IL sorbent.

Table 4.2 (cont.)

Samples	Ag species	Added (mg L ⁻¹)	Found (mg L ⁻¹)	Recovery (%)	RSD (%)
underground water	Au(III)	0	N.D.	-	-
		1	0.72 ± 0.02	71.71	2.79
	AuNPs (non-stabilizer)	0	N.D.	-	-
		1	0.23 ± 0.02	22.90	8.73
	Au(III)	0	N.D.	-	-
		1	0.72 ± 0.03	72.26	4.15
	AuNPs (citrate)	0	N.D.	-	-
		1	0.24 ± 0.02	24.38	8.20
	Au(III)	0	N.D.	-	-
		1	0.87 ± 0.01	86.86	1.15
	AuNPs (starch)	0	N.D.	-	-
		1	0.79 ± 0.01	78.60	1.07
	Au(III)	0	N.D.	-	-
		1	0.35 ± 0.02	35.26	5.67
	AuNPs (CTAB)	0	N.D.	-	-
		1	0.83 ± 0.02	83.25	2.40

Table 4.2 (cont.)

Samples	Ag species	Added (mg L ⁻¹)	Found (mg L ⁻¹)	Recovery (%)	RSD (%)
effluent	Au(III)	0	N.D.	-	-
		1	0.76 ± 0.02	75.53	2.78
	AuNPs (non-stabilizer)	0	N.D.	-	-
		1	0.15 ± 0.01	15.05	6.64
	Au(III)	0	N.D.	-	-
		1	0.74 ± 0.02	74.16	2.43
	AuNPs (citrate)	0	N.D.	-	-
		1	0.27 ± 0.02	27.45	7.29
	Au(III)	0	N.D.	-	-
		1	0.84 ± 0.01	83.99	1.19
	AuNPs (starch)	0	N.D.	-	-
		1	0.79 ± 0.01	78.70	1.27
	Au(III)	0	N.D.	-	-
		1	0.27 ± 0.03	27.42	10.94
	AuNPs (CTAB)	0	N.D.	-	-
		1	0.93 ± 0.02	92.98	2.15

N.D.: Not detected.

The proposed method was applied to extract and determine Au(III) ions and AuNPs by SiAP-IL with the optimum conditions chosen from the previous results and a spiked method was employed in this experiment. Real samples used in this work were jewelry wastewater collected from of the Gem and Jewelry Institute of Thailand, underground water collected from Khamphaeng Phet province, and an effluent collected from Thawi watthana district, Bangkok.

The analytical results are given in Table 4.2. It can be seen that Au(III) ions and AuNPs was found in the jewelry wastewater. The recovery of Au(III) was higher than 88% except for CTAB presence. Meanwhile, the recovery of AuNPs was higher

than 86% for starch and CTAB-stabilized AuNPs. The possible explanation for higher recovery of Au(III) for CTAB after elution procedure was due to the fact that Au(III) and AuNPs were trapped with positively charged CTAB surfactant. In case of underground water and effluent, Au(III) ions and AuNPs were not found. The higher recovery percentage for Au(III) was observed for all products except for the existence of CTAB stabilizer. Similarly with the jewelry wastewater results, the recovery of AuNPs was higher than 78% for starch and CTAB-stabilized AuNPs. The overall RSD are lower than 11 which in the acceptable range showed in Table 4.8. However, the higher recovery percentage was observed for binary mixture of Au(III) and starch stabilized-AuNPs in all samples with acceptable recovery.

4.7 Characterization of SiAP-HA

The procedure of SiAP-HA sorbent using humic acid immobilized onto aminopropyl solid sorbent is shown schematically in Figure 4.16. The synthesized SiAP-HA was characterized by FT-IR, surface area analysis and DR-UV-Vis compared with SiAP and HA.

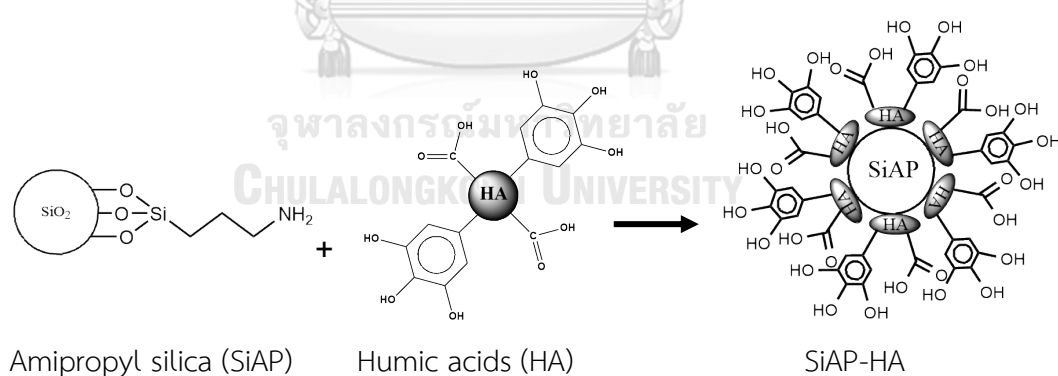


Figure 4.16 Schematic representation of HA immobilized onto SiAP.

4.7.1 Fourier transform infrared spectroscopy (FT-IR)

The infrared spectra of aminopropyl silica (SiAP), humic acids (HA) and humic acid immobilized on aminopropyl silica (SiAP-HA) were illustrated in Figure 4.17. The IR spectrum of HA shows an intense broad band around 3200-3500 cm^{-1} which generally refers to O-H stretching of carboxyl and phenolic groups. The small peaks around 2852 and 2920 cm^{-1} represent aliphatic C-H stretching. The peak around 1625 cm^{-1} is preferentially ascribed to C=O stretching and C=C stretching of aromatic group was found at 1640 cm^{-1} . The absorption spectra of HA modified SiAP exhibit the combination of HA spectra and SiAP spectra. This result showed that HA was successfully modified onto SiAP surface.

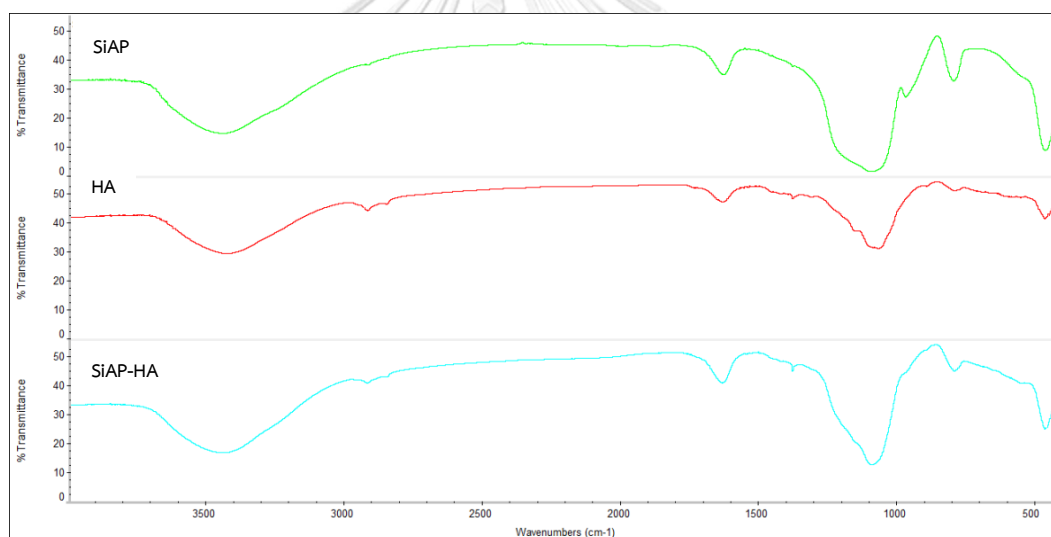


Figure 4.17 FT-IR spectra of aminopropyl silica (SiAP), humic acid (HA) and HA immobilized on aminopropyl silica (SiAP-HA).

4.7.2 Surface area analysis

The surface area and pore volume of adsorbents were studied by using BET surface area analysis (Table 4.3).

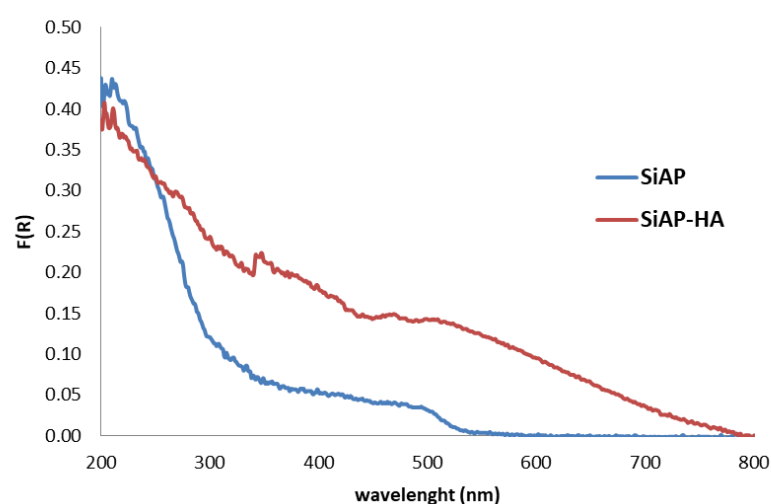
Table 4.3 Summary of the adsorbent parameters measured by surface area analysis

Adsorbent	BET surface area ($\text{m}^2 \text{g}^{-1}$)	Total pore volume ($\text{cm}^3 \text{g}^{-1}$)
SiAP	327.52	0.4075
SiAP-HA	99.667	0.2057

The results in Table 4.3 show that there is a change of surface area and pore volume of HA modified-SiAP. The surface area and pore volume was distinctly declined when SiAP was modified with HA. Therefore, this result supported that humic acids were successfully immobilized onto SiAP.

4.7.3 DR-UV-Vis

The solid sorbent of SiAP and SiAP-HA were characterized by DR-UV-Vis. The DR-UV-Vis spectra are shown in Figure 4.18.

**Figure 4.18** DR-UV-Vis spectra of SiAP and SiAP-HA.

After modification procedure, the contrary of white SiAP was changed to dark brown of SiAP-HA by visual observation. Moreover, the DR-UV-Vis signal of both adsorbents was also significantly different. It is well known that humic acid has a broad and featureless of UV-Vis spectrum. The absorption characteristic at 254 and

270-280 nm represented an organic matter content and total aromaticity, respectively, in humic acid structure. There was a few research studied on the characteristic of their brown color in visible region at 470, 570 and 620 nm [93, 94]. It is possible that carboxylic, phenolic and aromatic groups containing in HA structure can adsorb UV and Vis radiation as seen that $f(R)$ of SiAP-HA is obviously higher than that of SiAP.

4.8 Silver nanoparticles

In this work, silver nanoparticles with different stabilizers were characterized by TEM technique as showed in Figure 4.19. The TEM images of starch-AgNPs and citrate-AgNPs display typical shape of spherical particles with average diameter size of 50 to 200 nm.

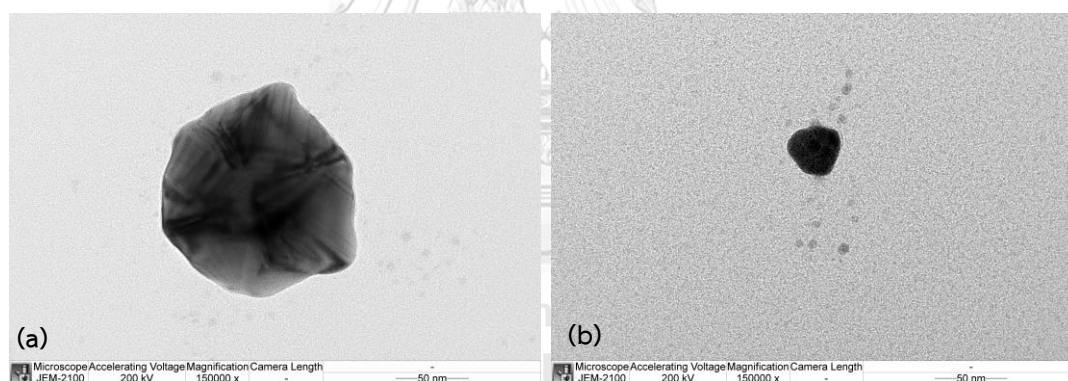


Figure 4.19 TEM images (150,000 × magnification) of (a) starch-AgNPs and (b) citrate-AgNPs.

4.9 Optimization of Ag ions/nanoparticles extraction

4.9.1 Effect of pH

The pH of solution affects dramatically to adsorption behavior of metals. Thus, the extraction of Ag(I) ions and AgNPs as a function of pH was studied by using SiAP-HA sorbent. The influence of pH on the extraction efficiency of Ag(I) and AgNPs was investigated in the pH range of 2-7 and the results are shown in Figure 4.20.

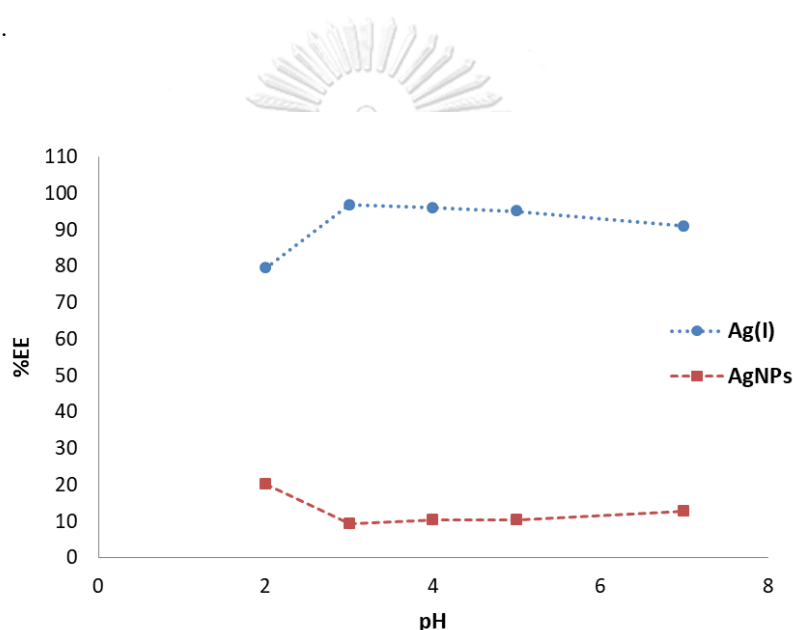


Figure 4.20 Effect of pH on the extraction of Ag(I) and AgNPs by SiAP-HA.

In this experiment, the extraction time was fixed at 60 minutes in order to ensure the adsorption equilibrium. The influence of acidic solution on the adsorption behavior of Ag(I) and AgNPs was investigated within pH range 2-7 because precipitation of silver oxide was occurred after adjusting pH higher than 7. It was found that the lowest extraction efficiency of Ag(I) was observed at pH 2 and rapidly rose with further pH increase. The surface of humic acids mainly composes of carboxylic group [95], it is possible that hydrogen ions at strongly acidic solution could be strived with Ag(I) cations and the protonation of the adsorbent surface functional group was occurred. This possibility would not be appropriate for Ag(I) ions

and probably restrict metal cations to bind with adsorbent surface. On the other hand at higher pH range of 3-7, the carboxylic group could be dissociated and the binding of Ag(I) cations and the negatively charge of carboxylate on HA surface was occurred [27]. The possible mechanism of Ag(I) cations with SiAP-HA was complexation and ion exchange [66, 96]. Meanwhile, the surface binding sites of SiAP-HA was not appropriated for AgNPs which inclined lower extraction efficiency in all pH range. Therefore, at pH value higher than 3 is preferable to separated Ag(I) ions and AgNPs in this research.

Moreover, the extraction efficiency of Ag(I) ions and AgNPs was also investigated using unmodified aminopropyl silica (SiAP) in order to compare the extraction performance with the modified-SiAP sorbent.

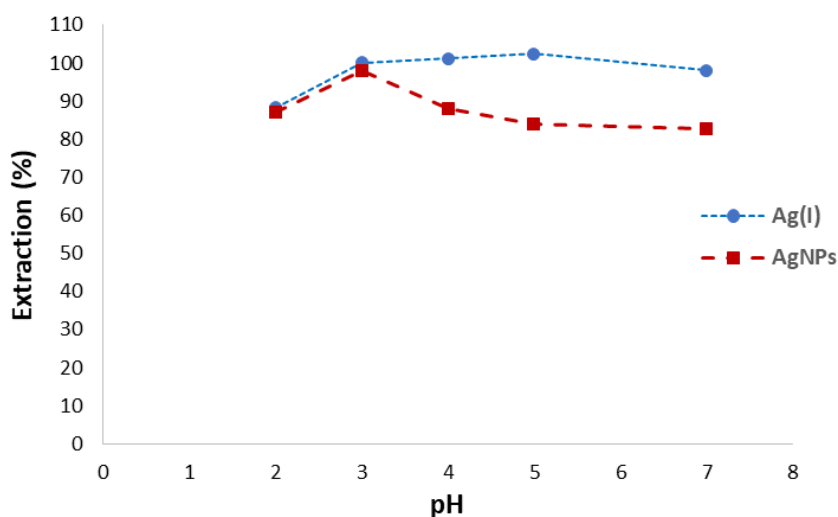


Figure 4.21 Effect of pH on the extraction of Ag(I) and AgNPs by SiAP.

The influence of pH on the extraction efficiency of Ag(I) ions and AgNPs is shown in Figure 4.21. The extraction time was also fixed at 60 minutes similarly to previous experiment using SiAP-HA adsorbent. The results show an increase of the extraction efficiency of Ag(I) when pH of solution increased, whereas the extraction efficiency of AgNPs was rapidly decreased at higher pH range. However, the separation behavior of Ag(I) and AgNPs with this adsorbent was not

significantly different at all pH range. Thus, the unmodified SiAP sorbent was not deserved for the separation of Ag(I) ions and AgNPs in this study.

4.9.2 Effect of time

The extraction efficiency of Ag(I) ions and AgNPs as a function of contact time was studied by employing SiAP-HA. The results are shown in Figure 4.22.

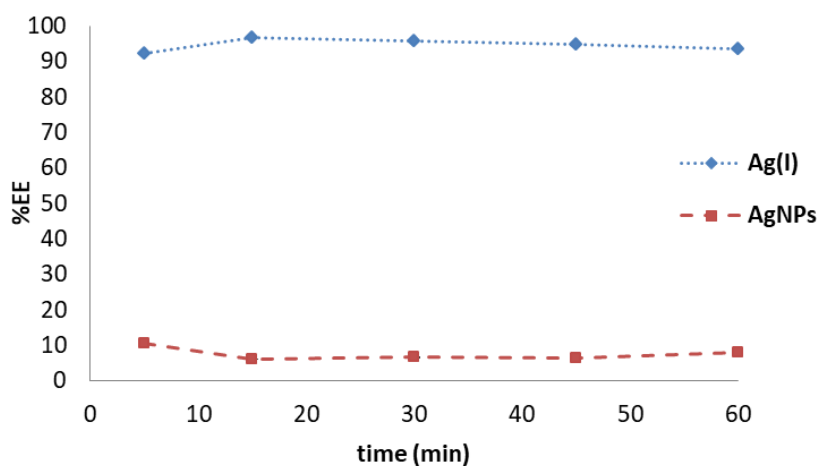


Figure 4.22 Effect of extraction time on the extraction of Ag(I) and AgNPs by SiAP-HA.

In this study, the extraction time was varied from 5 to 60 minutes at the optimum pH of 3 from previous experiment. The result obviously shows that AgNPs would unfavorable adsorbed onto humic acids surface over the time, whereas Ag(I) ions exhibit a great adsorption behavior. The adsorption of Ag(I) and AgNPs reached equilibrium within 15 minutes. Therefore, further studies were performed using an extraction time of 15 minutes.

4.10 Adsorption isotherm of Ag(I)

According to thoroughly low adsorption of AgNPs by SiAP-HA, this result could be described for Ag(I) ions. In this study, a comparison of Langmuir and Freundlich

models was investigated for the adsorption behavior of Ag(I) by SiAP-HA at pH 3 and 298 K by using equation 4.2 and 4.3. The adsorption isotherm experiments were evaluated by varying initial concentration of Ag(I) in the range of 10-300 mg L⁻¹ and stirring time was 15 min.

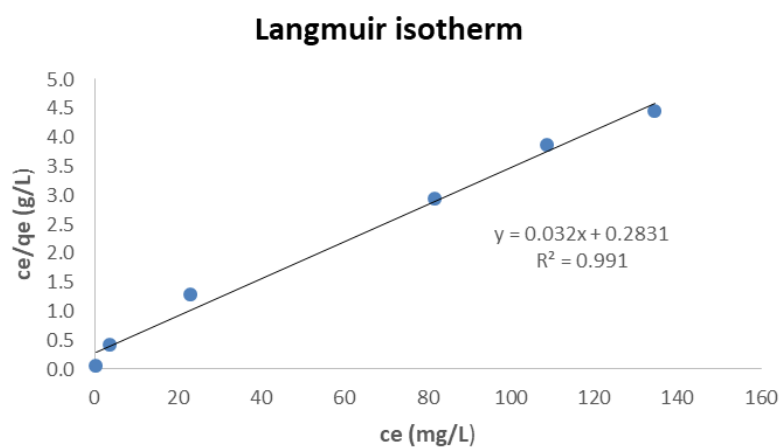


Figure 4.23 Langmuir isotherm of Ag(I) onto SiAP-HA.

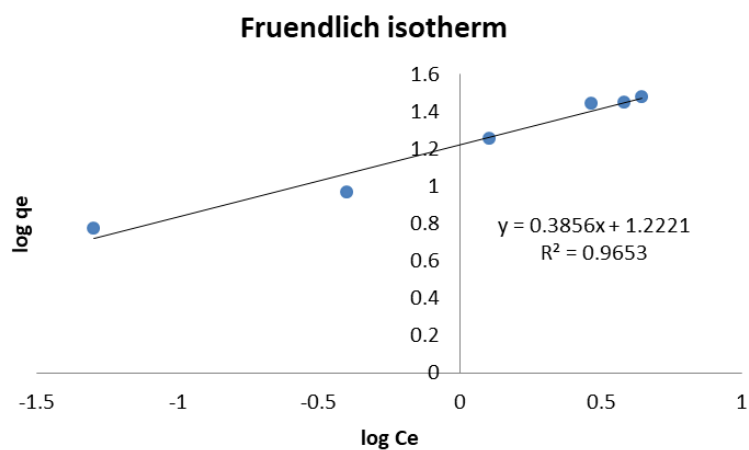


Figure 4.24 Fruendlich isotherm of Ag(I) onto SiAP-HA.

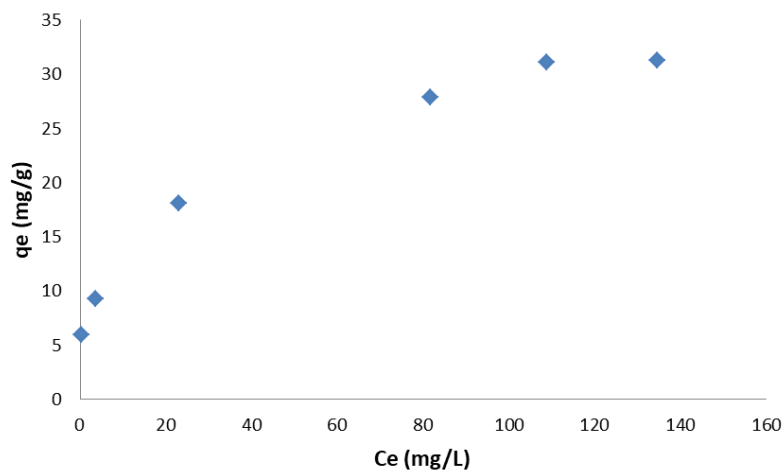


Figure 4.25 Adsorption isotherm of Ag(I) onto SiAP-HA.

The study of adsorption data in Figure 4.23 shows that the Langmuir model showed the best correlation with the experimental data when compared with the Freundlich model. The monolayer coverage of Ag(I) ions onto the SiAP-HA surface occurred with a maximum capacity of 31.3 mg g^{-1} . The calculated parameters, including K_L and R^2 are 0.11 L mg^{-1} and 0.9910 , respectively. Moreover, the adsorption isotherm behavior of Ag(I) ions onto SiAP-HA exhibited a plateau at around 31 mg g^{-1} in Figure 4.25 which consistent with a maximum capacity value from the Langmuir model.

4.11 Separation of Ag ions/nanoparticles

A binary mixture of Ag(I) and AgNPs solution was investigated onto SiAP-HA sorbent to consider a performance of metal separation. In this experiment, starch stabilized-AgNPs and citrate stabilized-AgNPs (Figure 4.26 (a) and (b), respectively) were used to compare extraction efficiency of the proposed method.

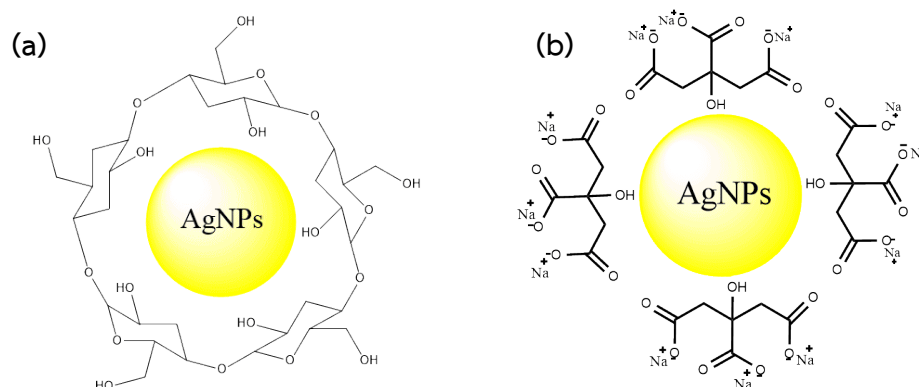


Figure 4.26 Schematic representations various types of stabilizer immobilized-AuNPs (a) starch and (b) tri-sodium citrate.

In order to separate AgNPs from Ag(I) ions using SiAP-HA adsorbent, solutions containing 5 mg L^{-1} of each metal at pH 3 were subjected to the optimal extraction time for 15 minutes. The results are shown in Figure 4.27 and 4.28 for starch stabilized-AgNPs and citrate stabilized-AgNPs, respectively. It was found that AgNPs show high recovery percentage for both stabilizers. This observation implied that starch stabilized-AgNPs and citrate stabilized-AgNPs were not suitable surface charge to bind with HA surface at pH 3. The proposed structures of both AgNPs are schematically shown in Figure 4.24. Moreover, the color of solution remained in pale-yellow for existence of both stabilizers of AgNPs after complete extraction. This result indicated that AgNPs was not adsorbed onto SiAP-HA surface.

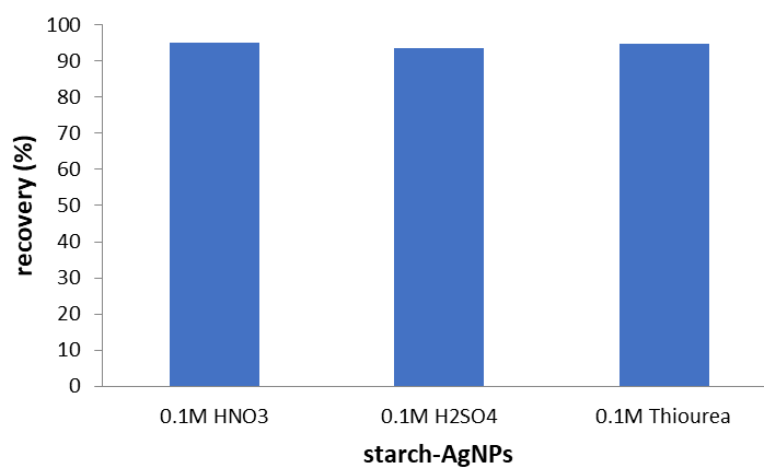


Figure 4.27 The recovery of starch stabilized-AgNPs by SiAP-HA.

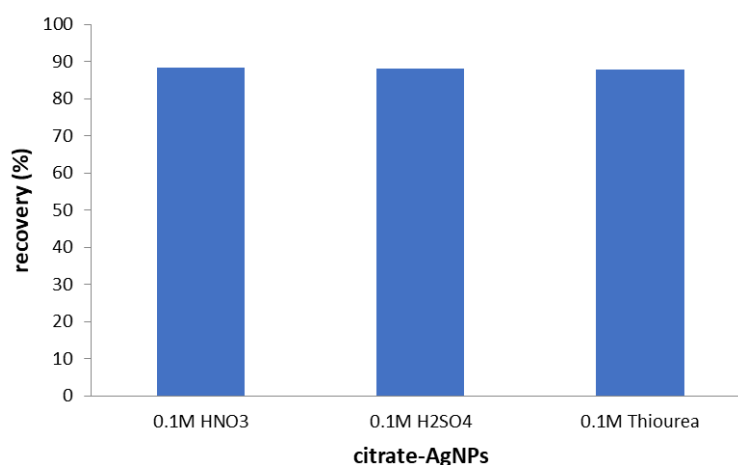


Figure 4.28 The recovery of tri-sodium citrate stabilized-AgNPs by SiAP-HA.

To determine Ag(I) ions adsorbed onto SiAP-HA, the optimal eluent for adsorbed metal was studied. The selectivity of eluents for Ag(I) was evaluated using HNO₃, H₂SO₄ and thiourea and the results are illustrated in Figure 4.29 and 4.30 for the existence of starch stabilized-AgNPs and citrate stabilized-AgNPs, respectively. The results show that HNO₃ and H₂SO₄ can quantitatively desorb Ag(I) ions with high efficiency, whereas lower elution percentage was observed when using thiourea. The higher elution efficiency of HNO₃ and H₂SO₄ was probably due to protons from acidic solution could expel the adsorbed metal cations as well as interrupted the chelation between metals ions and humic acids. Contrary to thiourea, the lowest elution percentage was gained. It is likely that thiourea (SCN₂H₄) containing preferably soft base ligand which feasible to bind with Ag(I) ions soft acid and thus thiourea molecule could be stuck on the sorbent surface with Ag(I) molecule.

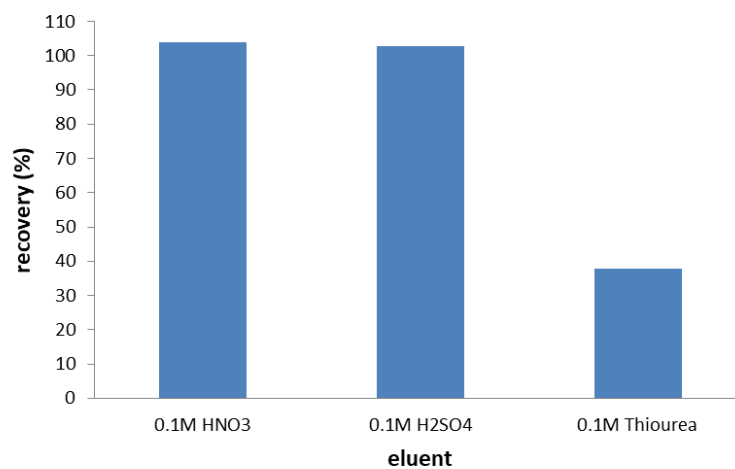


Figure 4.29 Elution of Ag(I) ions in the existence of starch-AgNPs using 0.1 M HNO₃, 0.1 M H₂SO₄ and 0.1 M Thiourea as eluents.

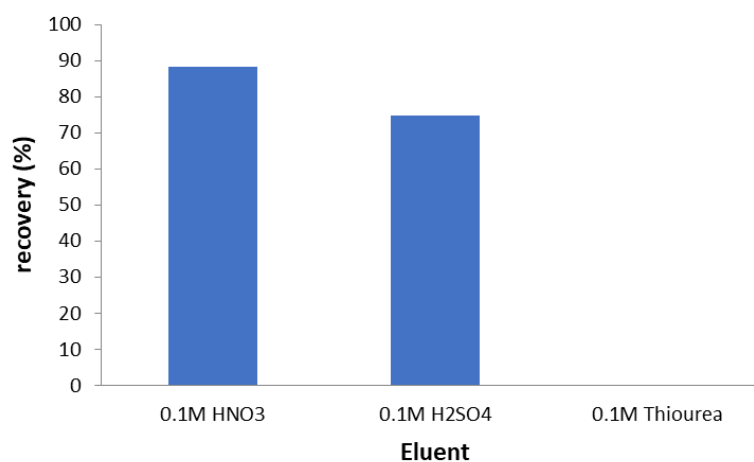


Figure 4.30 Elution of Ag(I) ions in the existence of citrate-AgNPs using 0.1 M HNO₃, 0.1 M H₂SO₄ and 0.1 M Thiourea as eluents.

4.12 Method validation

In this study, the determination of Ag(I) ions and AgNPs in real samples were quantified and reported in term of accuracy and precision. Furthermore, detection limit (LOD) was also studied.

Table 4.4 Analytical results of Ag(I) ions and AgNPs in sample (n=3).

Samples	Ag species	Added (mg L ⁻¹)	Found (mg L ⁻¹)	Recovery (%)	RSD (%)
Nano seven pet	Ag(I)	0	0.30 ± 0.01	-	-
		1	1.12 ± 0.01	81.37	1.17
	AgNPs	0	0.78 ± 0.00	-	-
		1	1.65 ± 0.01	86.43	0.37
Nanosilver Bact.	Ag(I)	0	0.32 ± 0.00	-	-
		1	1.21 ± 0.06	88.44	1.69
	AgNPs	0	0.94 ± 0.00	93.79 ^a	0.50

^a The recovery is estimated from the certified value of AgNPs of 1.00 mg L⁻¹

The proposed method was applied to determine Ag(I) ions and AgNPs in real sample by using optimum conditions from previous experiments. The spiked method was employed in this experiment. Real samples used in this work were collected from household products of the Nano seven pets (odor removal spray) and the Nanosilver product of Chulalongkorn University (for get rid of bacteria).

The analytical results are given in Table 4.4. It can be seen that Ag(I) ions was found in both products of silver nanoparticles. The recovery for AgNPs in samples was 86.43 and 93.79 %. The recovery of Ag(I) ions was 81.37 and 88.44 %. Moreover, overall RSD (%) are lower than 2. Thus, the accuracy and precision results are in the acceptable range which shows in Table 4.6. These results displayed a great potential application for separation and determination of silver species in real samples.

Moreover, detection limit (LOD) was calculated according to equation 4.6 and illustrated in Table 4.5.

Table 4.5 Detection limit (LOD) of the proposed method

Metal	Concentration ($\mu\text{g L}^{-1}$)
Au	5.77
Ag	4.61

4.13 Characterization of SiAP

In this work, SiAP sorbent was also investigated for separation of Ag(I) and AgNPs. The synthesized SiAP was characterized by FT-IR and surface area analysis compared with silica gel. The process of SiAP sorbent is shown schematically in Figure 4.31.

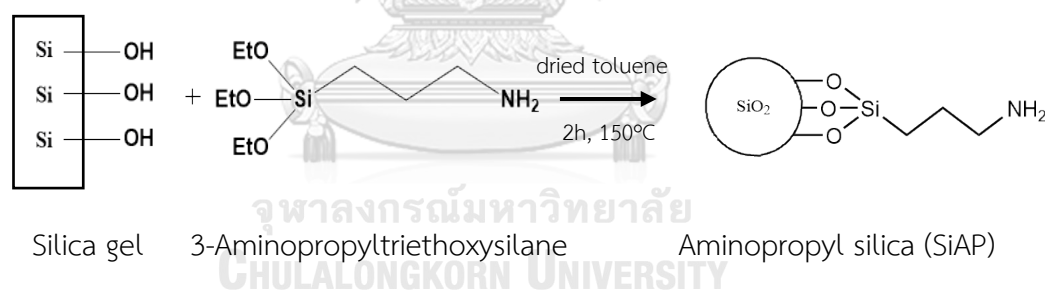


Figure 4.31 Schematic representation of SiAP synthesis.

4.13.1 Fourier transform infrared spectroscopy (FT-IR)

The SiAP and silica gel were characterized by FT-IR spectroscopy (Figure 4.32). The Si-O-Si stretching mode of silica gel can be observed as a strong peak at 1101 cm^{-1} and a broad band at 3501 cm^{-1} is belonging to Si-OH groups. The IR spectrum of the SiAP exhibits N-H stretching of amino groups ($3300\text{-}3600\text{ cm}^{-1}$),

aliphatic C-H stretching ($2846, 2920\text{ cm}^{-1}$), N-H stretching (1590 cm^{-1}), and C-N stretching (1095 cm^{-1}). This result showed that SiAP was successfully synthesized.

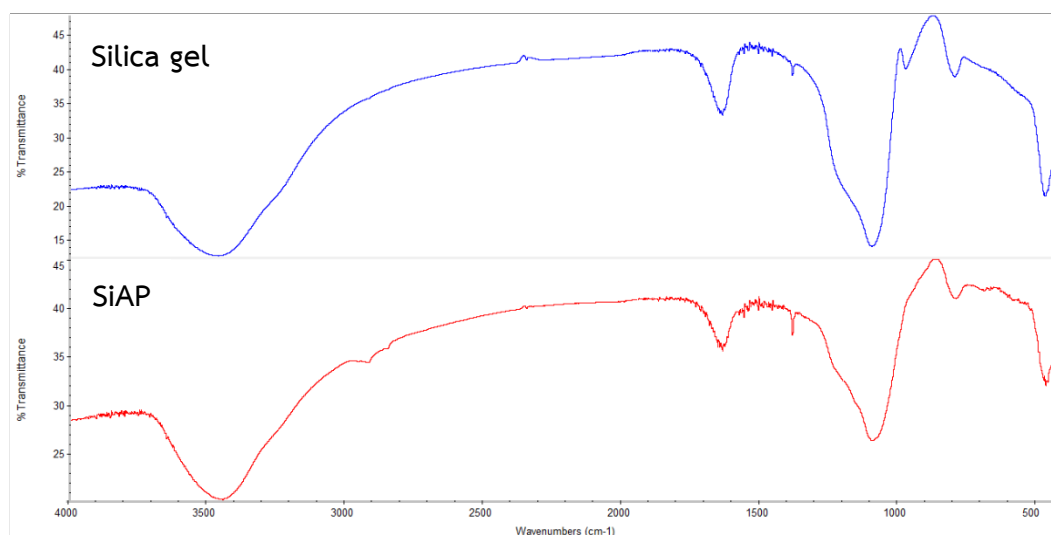


Figure 4.32 FT-IR spectra of silica gel and aminopropyl silica (SiAP).

4.13.2 Surface area analysis

The surface area and pore volume of adsorbents were investigated by using BET surface area analysis (Table 4.6).

Table 4.6 Summary of the adsorbent parameters measured by surface area analysis

Adsorbent	BET surface area ($\text{m}^2\text{ g}^{-1}$)	Total pore volume ($\text{cm}^3\text{ g}^{-1}$)
Silica gel	344.84	0.6455
SiAP	284.88	0.4075

The surface area and pore volume of the modified adsorbent were compared to the unmodified adsorbent (Table 4.6) by BET surface area analysis. The results showed that the surface area and total pore volume of the SiAP were obviously different from the unmodified silica gel. It is possible that the functionalized molecule was employed onto the surface as well as inside the pores of the adsorbent.

4.14 Optimization of Ag ions/nanoparticles extraction

4.14.1 Effect of pH

In this study, the effect of pH on the extraction of Ag(I) and AgNPs was evaluated and the results are shown in Figure 4.21. The extraction time was fixed at 60 minutes to ensure the adsorption equilibrium. It was found that when the pH values of the solution increased, the extraction efficiency of Ag(I) increased whereas the extraction efficiency of AgNPs decreased. At pH values more than 3, it is likely that the amine group on the adsorbent surface became negatively charges. Thus, the higher adsorption ability toward Ag^+ cations was occurred. Contrary for the decrease of adsorption ability at lower pH range ($\text{pH} < 3$) could be attributed to the protonation of the adsorbent surface which could not be appropriate for Ag cations affinity.

The extraction efficiency of AgNPs decreased when rising of pH value. As reported in the reviews proposed by Jasiorski et. al., the research on the deposition of AgNPs onto the silica-modified substrates showed that modification of silica surface with amine groups could be enhanced the attachment of AgNPs [97]. On the other hands, a smaller size of AgNPs formation was obtained at higher pH according to the findings of Alqadi et. al. [98]. This result suggesting that the particle sizes of AgNPs were not suitable for binding site with the adsorbent surface at higher pH range. However, transformation of AgNPs into Ag(I) ions was probably occurred due to oxidizing reagent of nitric acid in pH adjustment process. Therefore, the maximum sorption capacity of both metals onto the SiAP was obtained at pH 3.

4.14.2 Effect of time

The effect of extraction time of Ag(I) and AgNPs was studied. The results are shown in Figure 4.33 and demonstrated that the adsorption of Ag(I) and AgNPs at pH 3 onto SiAP appeared increase rapidly and reach equilibrium within 5

minutes. Thus, further studies were performed using an extraction time of 15 minutes to ensure the adsorption equilibrium was reached.

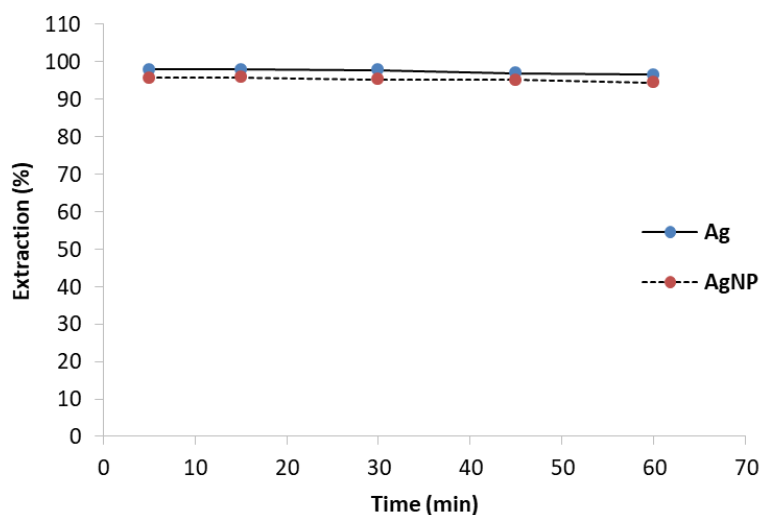


Figure 4.33 Effect of extraction time of Ag and AgNPs at pH 3 by SiAP.

4.15 Adsorption isotherm of Ag(I) and AgNPs

In this study, a comparison of Langmuir and Freundlich models was constructed for the adsorption phenomena of Ag(I) and AgNPs by SiAP at pH 3.0 and 298 K. The adsorption isotherm experiments were studied by varying the initial concentration of Ag(I) and AgNPs ($10\text{--}300\text{ mg L}^{-1}$) and the stirring time was 15 minutes. The Langmuir model was represented a monolayer sorption onto the homogeneous surface with a specific number of equivalent sites, according to equation 4.2. Meanwhile, the Freundlich model described multilayer sorption related to equation 4.3.

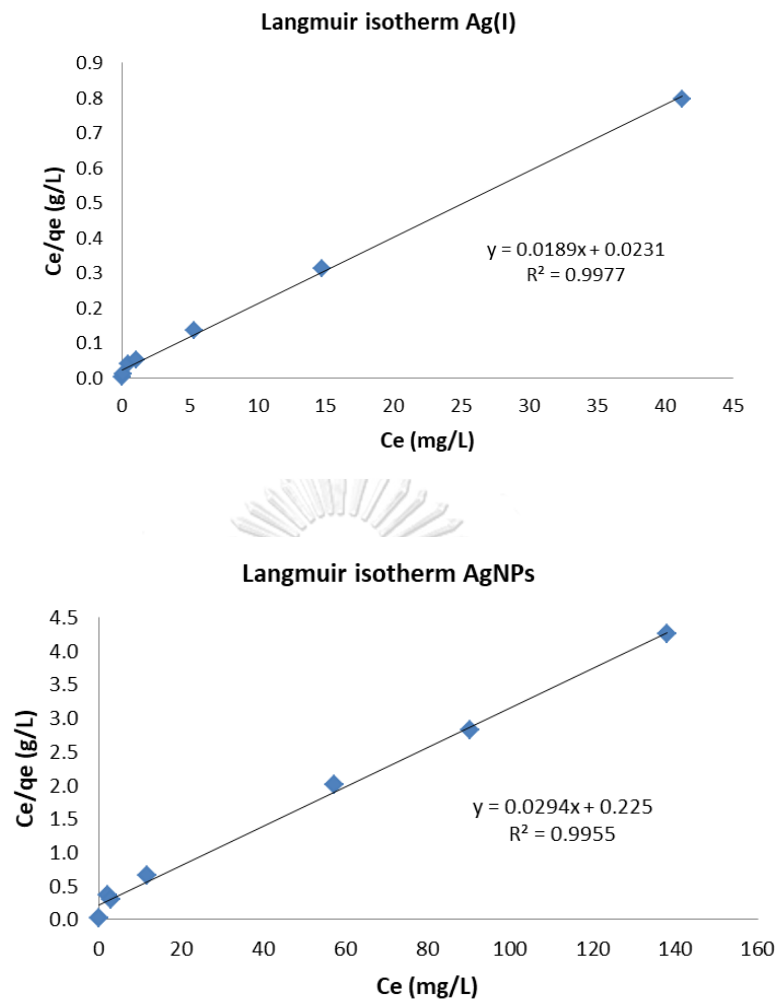


Figure 4.34 Langmuir isotherm of Ag(I) and AgNPs onto SiAP.

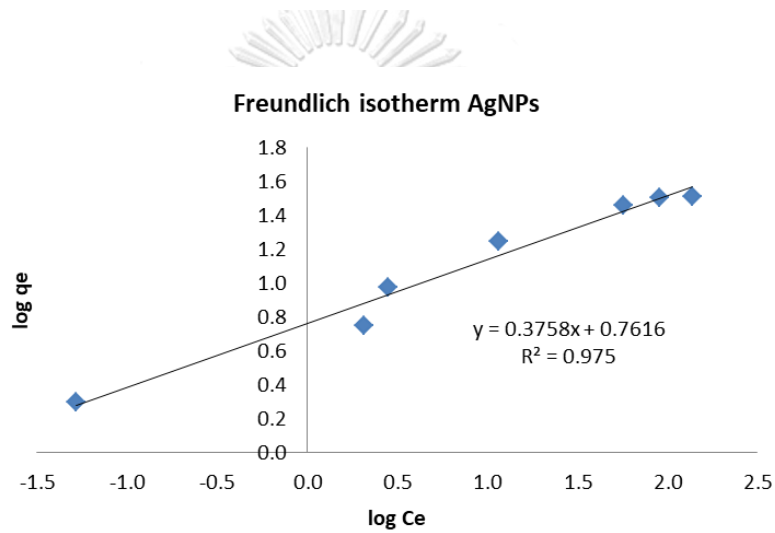
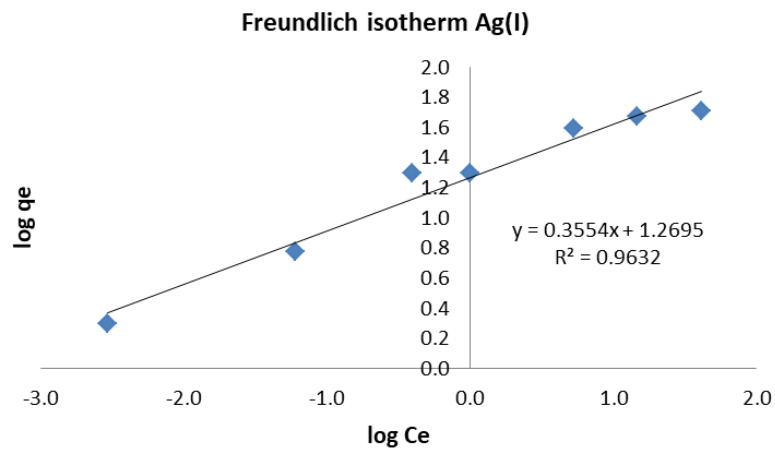
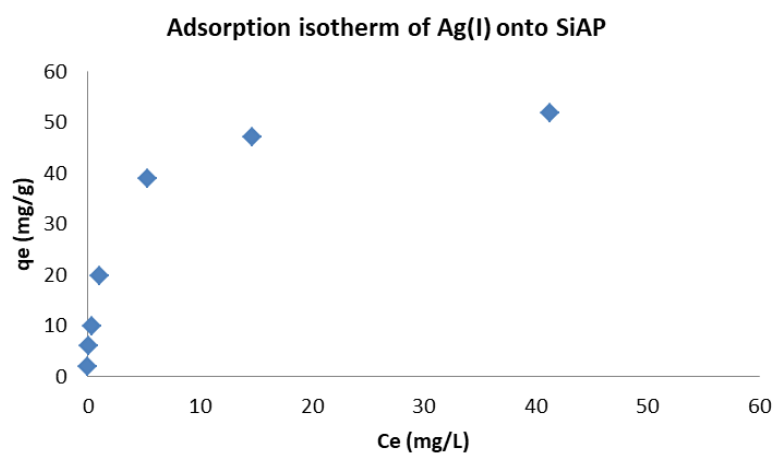


Figure 4.35 Freundlich isotherm of Ag(I) and AgNPs onto SiAP.



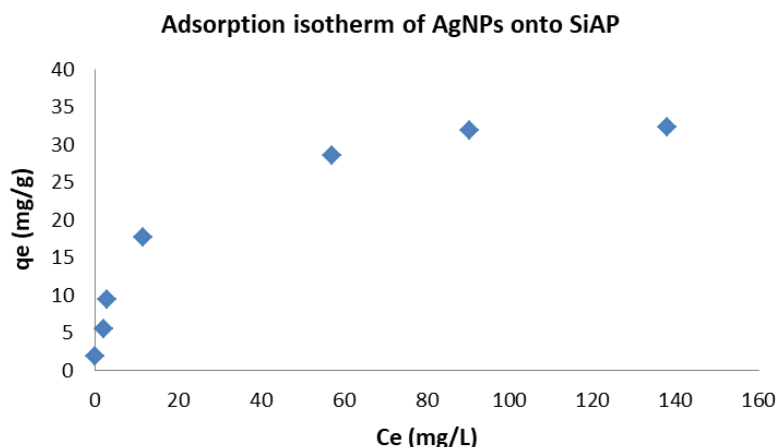


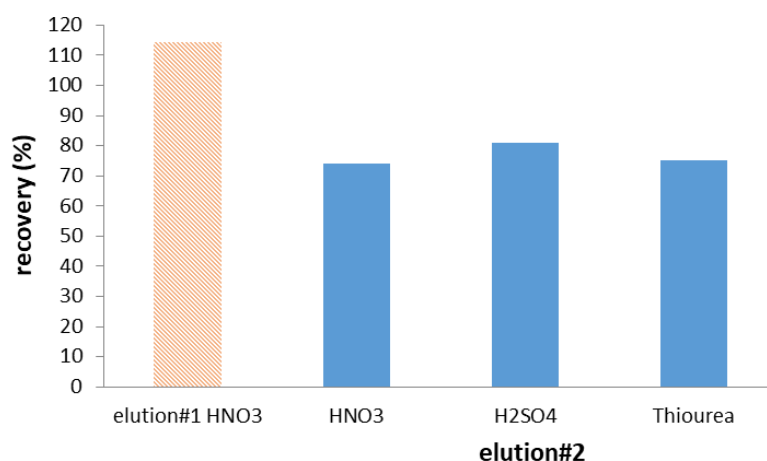
Figure 4.36 Adsorption isotherm of Ag(I) and AgNPs onto SiAP.

From these isotherms, the Langmuir model (Figure 4.34) showed the best correlation with the experimental data. The monolayer coverage of Ag(I) ions and AgNPs onto the SiAP surface occurred with a maximum capacity of 52.91 mg g^{-1} and 34.01 mg g^{-1} , respectively. Furthermore, the adsorption isotherm behavior of Ag(I) and AgNPs onto SiAP in Figure 4.36 showed metal adsorbed on the adsorbent was reached a plateau at around 52 and 34 mg g^{-1} consistent with a maximum capacity value from the Langmuir model.

4.16 Sequential elution of Ag(I) and AgNPs

The selectivity of eluents for the sequential elution of binary mixtures containing Ag(I) and AgNPs was further examined using various types of eluents and the results are given in Figure 4.37. The solutions contained 5 mg L^{-1} of each metal (pH 3) and subjected to the optimal extraction procedure (15 minutes). To separate Ag and AgNPs, 0.1M HNO_3 , 0.1M H_2SO_4 , and 0.1M Thiourea were used for the desorption of these metals from the adsorbent after extraction procedure. The elution process was divided into 2 steps, each for 15 minutes. The first step, SiAP were soaked with each eluent in order to obtain Ag(I) ions. Followed by using 2 % (v/v) H_2O_2 to oxidize remaining AgNPs on the adsorbent and eluted again with each eluent.

It was found that three eluents can quantitatively desorb Ag(I) ions with higher recovery (>90%) in the first step of elution. This indicates a displacement of protons from HNO₃ and H₂SO₄ to the adsorbed Ag(I) ions, thus the binding ability of Ag(I) ions with the amino groups of adsorbents was interrupted. In case of thiourea, a possible desorption mechanism is to form a stable complex with Ag(I) ions. Moreover, the mixture solution of Ag(I) ions and AgNPs resulted in the change of color from yellow to colorless. Meanwhile, the color of SiAP adsorbent was changed from white to yellow. This observation indicated that AgNPs were adsorbed onto the adsorbent. Among the eluents, thiourea showed the highest degree (>90%) of desorption over HNO₃ and H₂SO₄ in the second step, especially for employing after thiourea in the first step. Ag(I) species can be effectively eluted through thiourea elution was probably due to a stable form of Ag(I) ions and SCN₂H₄. Therefore, thiourea was chosen for sequential desorption of Ag(I) ions and AgNPs in further experiments.



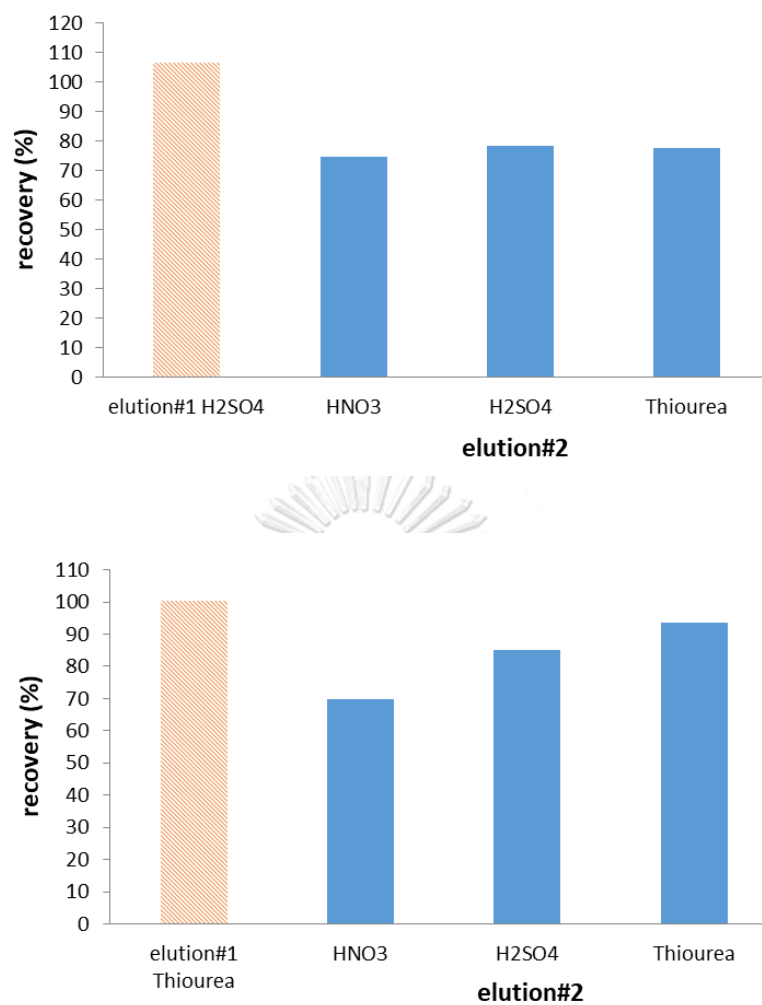


Figure 4.37 Elution of Ag(I) and AgNPs by varying eluents (0.1M HNO₃, 0.1M H₂SO₄ and 0.1M Thiourea).

4.17 Method validation

In this study, the determination of Ag(I) ions and AgNPs in real samples were quantified and reported in term of accuracy and precision.

Table 4.7 Analytical results of Ag(I) ions and AgNPs in sample (n=3).

Samples	Ag species	Added (mg L ⁻¹)	Found (mg L ⁻¹)	Recovery (%)	RSD (%)
Nano seven pet	Ag(I)	0	0.26 ± 0.01	-	-
		1	1.09 ± 0.02	83.51	1.84
	AgNPs	0	0.69 ± 0.01	-	-
1		1.59 ± 0.04	89.68	2.67	
Nanosilver Bact.	Ag(I)	0	0.27 ± 0.01	-	-
		1	1.13 ± 0.02	85.84	1.71
	AgNPs	0	0.87 ± 0.01	94.37 ^a	1.41

^a The recovery is estimated from the certified value of AgNPs of 1.00 mg L⁻¹

The proposed method was applied to determine Ag(I) ions and AgNPs in real sample by using optimum conditions from previous experiments. The spiked method was employed in this experiment. Real samples used in this work were collected from household products of Nano seven pet spray (for odor removal) and Nanosilver product of Chulalongkorn University (for get rid of bacteria). The analytical results are given in Table 4.7 and showed that Ag(I) ions was found in both products of silver nanoparticles. The recovery for AgNPs in samples was 89.68 and 94.37 %. The recovery of Ag(I) ions was 83.51 and 85.84 %. Moreover, overall RSD (%) are lower than 3. Thus, the accuracy and precision results are in the acceptable range which shows in Table 4.8. These results displayed a great potential application of the proposed method for separation and determination of silver species in real samples.

The acceptable analyte recovery and RSD at different concentrations are shown in Table 4.8.

Table 4.8 Analyte recovery and precision at different concentration [99].

Analyte (%)	Analyte ratio	Unit	Mean recovery (%)	RSD (%)
100	1	100 %	98-102	1.3
10	10-1	10 %	98-102	2.8
1	10-2	1 %	97-103	2.7
0.1	10-3	0.1 %	95-105	3.7
0.01	10-4	100 ppm	90-107	5.3
0.001	10-5	10 ppm	80-110	7.3
0.0001	10-6	1 ppm	80-110	11
0.00001	10-7	100 ppb	80-110	15
0.000001	10-8	10 ppb	60-115	21
0.0000001	10-9	1 ppb	40-120	30



CHARTER V

CONCLUSION

5.1 Conclusion

In this research, 1-carboxymethyl-3-methylimidazolium chloride ionic liquid [MimCM]Cl and humic acids (HA) immobilized onto aminopropyl silica (SiAP) sorbent was successfully prepared with a maximum capacity of 28.3 and 31.3 mg g⁻¹, respectively. These adsorbents were employed for the separation of gold and silver ions/nanoparticles in aqueous solution. The proposed method was profitable for the determination of gold and silver species via ICP-OES at optimum conditions. The acidic pH range of 3 was chosen to apply the optimum pH condition to the solution throughout this study. As for optimum extraction time, gold ions/nanoparticles showed a great adsorption behavior within 5 minutes whereas a good ability of silver ions/nanoparticles adsorption was observed within 15 minutes. The use of SiAP-ILs and SiAP-HA adsorbent can separate silver and gold ions/nanoparticles. Moreover, these adsorbents showed a good potential over unmodified-aminopropyl silica. Thiourea and HNO₃ were considered as a suitable eluent for gold ions and silver ions, respectively, from the adsorbent. However, aminopropyl silica (SiAP) sorbent was also studied for separation of Ag(I) and AgNPs. SiAP was successfully prepared with maximum capacity of 52.9 and 34.0 mg g⁻¹ for Ag(I) and AgNPs, respectively. The optimum extraction time was observed within 15 minutes and the sequential elution of silver species was achieved at pH 3.

The validation results for separation and determination of gold and silver ions/nanoparticles in real samples using modified-SiAP showed a good accuracy and precision for metal ions. The recovery of Au(III) ions was higher than 80% in the existence of starch stabilizer. The recovery of Ag(I) ions was 81.37 and 88.44%. The overall RSD are lower than 2. Meanwhile, the recovery for starch-AuNPs was 86.4, 78.60 and 78.70%. The recovery starch-AgNPs in samples was 86.43 and 93.79%. Moreover, SiAP also showed a good accuracy and precision for metal species. The

recovery of Ag(I) ions was 83.51 and 85.84%. The recovery starch-AgNPs in samples was 89.68 and 94.37%. The overall RSD are lower than 3. These accuracy and precision results of metal nanoparticles are in the acceptable range which calculated as relative standard (%RSD) is less than 3%. The detection limit (LOD) was 5.77 and 4.61 $\mu\text{g L}^{-1}$ for gold and silver, respectively, using ICP-OES. In this work, SiAP-HA was displayed a good potential and ease of procedure to separate Ag species over SiAP. Therefore, SiAP-ILs and SiAP-HA were achieved applied to separate and to determine gold and silver species in water samples and household products using ICP-OES which is simple, reliable, economical, and easy-to-use.

5.2 Suggestions for future work

- This proposed method should be studied further for the matrix compositions of wastewater and household products.
- The modified aminopropyl silica adsorbent should be studied further in column system in order to obtain a comfortable system and apply in other kinds of sample.
- This proposed method should be studied further for preconcentration of metal species prior to analysis.

REFERENCES

- [1] Fabrega, J., Luoma, S.N., Tyler, C.R., Galloway, T.S., and Lead, J.R. Silver nanoparticles: behaviour and effects in the aquatic environment. Environment international 37(2) (2011): 517-531.
- [2] Zook, J.M., Long, S.E., Cleveland, D., Geronimo, C.L.A., and MacCuspie, R.I. Measuring silver nanoparticle dissolution in complex biological and environmental matrices using UV-visible absorbance. Analytical and bioanalytical chemistry 401(6) (2011): 1993.
- [3] Ramos, K., Gómez-Gómez, M., Cámara, C., and Ramos, L. Silver speciation and characterization of nanoparticles released from plastic food containers by single particle ICPMS. Talanta 151 (2016): 83-90.
- [4] Epstein, M., Emri, I., Hartemann, P., Hoet, P., Leitgeb, N., and Martínez Martínez, L. Scientific Committee on Emerging and Newly Identified Health Risks (SCENIHR). Opinion on Nanosilver: safety, health and environmental effects and role in antimicrobial resistance (2014).
- [5] Speranza, A., Leopold, K., Maier, M., Taddei, A.R., and Scoccianti, V. Pd-nanoparticles cause increased toxicity to kiwifruit pollen compared to soluble Pd (II). Environmental pollution 158(3) (2010): 873-882.
- [6] Navarro, E., et al. Toxicity of silver nanoparticles to *Chlamydomonas reinhardtii*. Environmental science & technology 42(23) (2008): 8959-8964.
- [7] Reidy, B., Haase, A., Luch, A., Dawson, K.A., and Lynch, I. Mechanisms of silver nanoparticle release, transformation and toxicity: a critical review of current knowledge and recommendations for future studies and applications. Materials 6(6) (2013): 2295-2350.
- [8] Yu, S.-j., Yin, Y.-g., and Liu, J.-f. Silver nanoparticles in the environment. Environmental Science: Processes & Impacts 15(1) (2013): 78-92.
- [9] Ngeontae, W., Janrungratsakul, W., Morakot, N., Aeungmaitrepirom, W., and Tuntulani, T. New silver selective electrode fabricated from benzothiazole

- calix [4] arene: speciation analysis of silver nanoparticles. Sensors and Actuators B: Chemical 134(2) (2008): 377-385.
- [10] López-Lorente, A., Simonet, B., and Valcárcel, M. Electrophoretic methods for the analysis of nanoparticles. TrAC Trends in Analytical Chemistry 30(1) (2011): 58-71.
- [11] Von der Kammer, F., et al. Analysis of engineered nanomaterials in complex matrices (environment and biota): general considerations and conceptual case studies. Environmental Toxicology and Chemistry 31(1) (2012): 32-49.
- [12] Soto-Alvaredo, J., Montes-Bayón, M.a., and Bettmer, J.r. Speciation of silver nanoparticles and silver (I) by reversed-phase liquid chromatography coupled to ICPMS. Analytical chemistry 85(3) (2013): 1316-1321.
- [13] Wu, N., Wyart, Y., Liu, Y., Rose, J., and Moulin, P. An overview of solid/liquid separation methods and size fractionation techniques for engineered nanomaterials in aquatic environment. Environmental Technology Reviews 2(1) (2013): 55-70.
- [14] Fabricius, A.-L., Duester, L., Meermann, B., and Ternes, T.A. ICP-MS-based characterization of inorganic nanoparticles—sample preparation and off-line fractionation strategies. Analytical and bioanalytical chemistry 406(2) (2014): 467-479.
- [15] Franze, B. and Engelhard, C. Fast separation, characterization, and speciation of gold and silver nanoparticles and their ionic counterparts with micellar electrokinetic chromatography coupled to ICP-MS. Analytical chemistry 86(12) (2014): 5713-5720.
- [16] López-García, I., Vicente-Martínez, Y., and Hernández-Córdoba, M. Speciation of silver nanoparticles and Ag (I) species using cloud point extraction followed by electrothermal atomic absorption spectrometry. Spectrochimica Acta Part B: Atomic Spectroscopy 101 (2014): 93-97.
- [17] Proulx, K. and Wilkinson, K.J. Separation, detection and characterisation of engineered nanoparticles in natural waters using hydrodynamic chromatography and multi-method detection (light scattering, analytical

- ultracentrifugation and single particle ICP-MS). Environmental Chemistry 11(4) (2014): 392-401.
- [18] Ali, I. and Gupta, V. Advances in water treatment by adsorption technology. Nature protocols 1(6) (2006): 2661.
- [19] Gupta, V., Carrott, P., Ribeiro Carrott, M., and Suhas. Low-cost adsorbents: growing approach to wastewater treatment—a review. Critical Reviews in Environmental Science and Technology 39(10) (2009): 783-842.
- [20] Huddleston, J.G., Visser, A.E., Reichert, W.M., Willauer, H.D., Broker, G.A., and Rogers, R.D. Characterization and comparison of hydrophilic and hydrophobic room temperature ionic liquids incorporating the imidazolium cation. Green chemistry 3(4) (2001): 156-164.
- [21] Freemantle, M. Designer solvents-Ionic liquids may boost clean technology development. Chemical & engineering news 76(13) (1998): 32-37.
- [22] Vidal, L., Parshintsev, J., Hartonen, K., Canals, A., and Riekkola, M.-L. Ionic liquid-functionalized silica for selective solid-phase extraction of organic acids, amines and aldehydes. Journal of chromatography A 1226 (2012): 2-10.
- [23] Vidal, L., Riekkola, M.-L., and Canals, A. Ionic liquid-modified materials for solid-phase extraction and separation: a review. Analytica chimica acta 715 (2012): 19-41.
- [24] Liang, M., Khatun, S., and Castner Jr, E.W. Communication: Unusual structure and transport in ionic liquid-hexane mixtures. 2015, AIP Publishing.
- [25] Steelink, C. What is humic acid? 1963, ACS Publications.
- [26] Ghabbour, E.A., Shaker, M., El-Toukhy, A., Abid, I.M., and Davies, G. Thermodynamics of metal cation binding by a solid soil-derived humic acid: Binding of Fe (III), Pb (II), and Cu (II). Chemosphere 63(3) (2006): 477-483.
- [27] Nadeem, R., Hanif, M.A., Mahmood, A., Jamil, M.S., and Ashraf, M. Biosorption of Cu (II) ions from aqueous effluents by blackgram bran (BGB). Journal of hazardous materials 168(2-3) (2009): 1622-1625.
- [28] Su, S., Chen, B., He, M., Xiao, Z., and Hu, B. A novel strategy for sequential analysis of gold nanoparticles and gold ions in water samples by combining magnetic solid phase extraction with inductively coupled plasma mass

- spectrometry. Journal of Analytical Atomic Spectrometry 29(3) (2014): 444-453.
- [29] Daniel, M.-C. and Astruc, D. Gold nanoparticles: assembly, supramolecular chemistry, quantum-size-related properties, and applications toward biology, catalysis, and nanotechnology. Chemical reviews 104(1) (2004): 293-346.
- [30] Kimling, J., Maier, M., Okenve, B., Kotaidis, V., Ballot, H., and Plech, A. Turkevich method for gold nanoparticle synthesis revisited. The Journal of Physical Chemistry B 110(32) (2006): 15700-15707.
- [31] Eustis, S. and El-Sayed, M.A. Why gold nanoparticles are more precious than pretty gold: noble metal surface plasmon resonance and its enhancement of the radiative and nonradiative properties of nanocrystals of different shapes. Chemical society reviews 35(3) (2006): 209-217.
- [32] Blaser, S.A., Scheringer, M., MacLeod, M., and Hungerbühler, K. Estimation of cumulative aquatic exposure and risk due to silver: contribution of nano-functionalized plastics and textiles. Science of the total environment 390(2-3) (2008): 396-409.
- [33] El-Nour, K.M.A., Eftaiha, A.a., Al-Warthan, A., and Ammar, R.A. Synthesis and applications of silver nanoparticles. Arabian journal of chemistry 3(3) (2010): 135-140.
- [34] Cushen, M., Kerry, J., Morris, M., Cruz-Romero, M., and Cummins, E. Nanotechnologies in the food industry—Recent developments, risks and regulation. Trends in Food Science & Technology 24(1) (2012): 30-46.
- [35] Badawy, A.M.E., Luxton, T.P., Silva, R.G., Scheckel, K.G., Suidan, M.T., and Tolaymat, T.M. Impact of environmental conditions (pH, ionic strength, and electrolyte type) on the surface charge and aggregation of silver nanoparticles suspensions. Environmental science & technology 44(4) (2010): 1260-1266.
- [36] Ramkumar, V.S., et al. Biofabrication and characterization of silver nanoparticles using aqueous extract of seaweed *Enteromorpha compressa* and its biomedical properties. Biotechnology reports 14 (2017): 1-7.

- [37] Choi, S.Y., et al. In vitro toxicity of serum protein-adsorbed citrate-reduced gold nanoparticles in human lung adenocarcinoma cells. Toxicology in vitro 26(2) (2012): 229-237.
- [38] Schaeublin, N.M., et al. Does shape matter? Bioeffects of gold nanomaterials in a human skin cell model. Langmuir 28(6) (2012): 3248-3258.
- [39] Sun, H., Jia, J., Jiang, C., and Zhai, S. Gold Nanoparticle-Induced Cell Death and Potential Applications in Nanomedicine. International journal of molecular sciences 19(3) (2018): 754.
- [40] AshaRani, P., Low Kah Mun, G., Hande, M.P., and Valiyaveetil, S. Cytotoxicity and genotoxicity of silver nanoparticles in human cells. ACS nano 3(2) (2008): 279-290.
- [41] Asharani, P., Wu, Y.L., Gong, Z., and Valiyaveetil, S. Toxicity of silver nanoparticles in zebrafish models. Nanotechnology 19(25) (2008): 255102.
- [42] Sweeney, S.F., Woehrle, G.H., and Hutchison, J.E. Rapid purification and size separation of gold nanoparticles via diafiltration. Journal of the American Chemical Society 128(10) (2006): 3190-3197.
- [43] Liu, J.-f., Yu, S.-j., Yin, Y.-g., and Chao, J.-b. Methods for separation, identification, characterization and quantification of silver nanoparticles. TrAC Trends in Analytical Chemistry 33 (2012): 95-106.
- [44] Li, L., Leopold, K., and Schuster, M. Effective and selective extraction of noble metal nanoparticles from environmental water through a noncovalent reversible reaction on an ionic exchange resin. Chemical Communications 48(73) (2012): 9165-9167.
- [45] Li, L. and Leopold, K. Ligand-assisted extraction for separation and preconcentration of gold nanoparticles from waters. Analytical chemistry 84(10) (2012): 4340-4349.
- [46] Sperling, R.A. and Parak, W.J. Surface modification, functionalization and bioconjugation of colloidal inorganic nanoparticles. Philosophical Transactions of the Royal Society of London A: Mathematical, Physical and Engineering Sciences 368(1915) (2010): 1333-1383.

- [47] Goto, K., Taguchi, S., Fukue, Y., Ohta, K., and Watanabe, H. Spectrophotometric determination of manganese with 1-(2-pyridylazo)-2-naphthol and a non-ionic surfactant. Talanta 24(12) (1977): 752-753.
- [48] Camel, V. Solid phase extraction of trace elements. Spectrochimica Acta Part B: Atomic Spectroscopy 58(7) (2003): 1177-1233.
- [49] Mahmoud, M.E., El-Essawi, M.M., Kholeif, S.A., and Fathalla, E.M. Aspects of surface modification, structure characterization, thermal stability and metal selectivity properties of silica gel phases-immobilized-amine derivatives. Analytica chimica acta 525(1) (2004): 123-132.
- [50] Safarik, I., Horska, K., Pospiskova, K., and Safarikova, M. Magnetic techniques for the detection and determination of xenobiotics and cells in water. Analytical and bioanalytical chemistry 404(4) (2012): 1257-1273.
- [51] Menezes, M., Moreira, J., and Campos, J. Adsorption of various ions from acetone and ethanol on silica gel modified with 2-, 3-, and 4-aminobenzoate. Journal of colloid and interface science 179(1) (1996): 207-210.
- [52] Sarkar, M., Datta, P.K., and Das, M. Equilibrium studies on the optimization of solid-phase extraction using modified silica gel for removal, recovery, and enrichment prior to the determination of some metal ions from aqueous samples of different origin. Industrial & engineering chemistry research 41(26) (2002): 6745-6750.
- [53] Ngeontae, W., Aeungmaitrepirom, W., Tuntulani, T., and Imyim, A. Highly selective preconcentration of Cu (II) from seawater and water samples using amidoamidoxime silica. Talanta 78(3) (2009): 1004-1010.
- [54] Pérez-Quintanilla, D., Sánchez, A., and Sierra, I. Preparation of hybrid organic-inorganic mesoporous silicas applied to mercury removal from aqueous media: Influence of the synthesis route on adsorption capacity and efficiency. Journal of colloid and interface science 472 (2016): 126-134.
- [55] Kvitck, R.J., Evans, J.F., and Carr, P.W. Diamine/Silane-Modified controlled pore glass: The covalent attachment reaction from aqueous solution and the mechanism of reaction of bound diamine with copper (II). Analytica Chimica Acta 144 (1982): 93-106.

- [56] Mahmoud, M.E. COMPARISON OF METAL SORPTION PROPERTIES OF THREE SILICA GEL PHASES—PHYSICALLY ADSORBED AND CHEMICALLY IMMOBILIZED-1-AMINOANTHRAQUINONE. Analytical Letters 35(7) (2002): 1251-1267.
- [57] Akl, M., Kenawy, I., and Lasheen, R. Organically modified silica gel and flame atomic absorption spectrometry: employment for separation and preconcentration of nine trace heavy metals for their determination in natural aqueous systems. Microchemical Journal 78(2) (2004): 143-156.
- [58] Soliman, E.M., Mahmoud, M.E., and Ahmed, S.A. Synthesis, characterization and structure effects on selectivity properties of silica gel covalently bonded diethylenetriamine mono-and bis-salicylaldehyde and naphthaldehyde Schiff, s bases towards some heavy metal ions. Talanta 54(2) (2001): 243-253.
- [59] Bois, L., Bonhommé, A., Ribes, A., Pais, B., Raffin, G., and Tessier, F. Functionalized silica for heavy metal ions adsorption. Colloids and Surfaces A: Physicochemical and Engineering Aspects 221(1-3) (2003): 221-230.
- [60] Li, M., Pham, P.J., Wang, T., Pittman Jr, C.U., and Li, T. Selective extraction and enrichment of polyunsaturated fatty acid methyl esters from fish oil by novel π -complexing sorbents. Separation and Purification Technology 66(1) (2009): 1-8.
- [61] Tian, M., Bi, W., and Row, K.H. Solid-phase extraction of liquiritin and glycyrrhizic acid from licorice using ionic liquid-based silica sorbent. Journal of separation science 32(23-24) (2009): 4033-4039.
- [62] Tian, M., Yan, H., and Row, K.H. Solid-phase extraction of tanshinones from *Salvia Miltiorrhiza* Bunge using ionic liquid-modified silica sorbents. Journal of Chromatography B 877(8-9) (2009): 738-742.
- [63] Fang, G., Chen, J., Wang, J., He, J., and Wang, S. N-Methylimidazolium ionic liquid-functionalized silica as a sorbent for selective solid-phase extraction of 12 sulfonylurea herbicides in environmental water and soil samples. Journal of chromatography A 1217(10) (2010): 1567-1574.
- [64] Tian, M., Bi, W., and Row, K.H. Molecular imprinting in ionic liquid-modified porous polymer for recognitive separation of three tanshinones from *Salvia*

- miltiorrhiza Bunge. Analytical and bioanalytical chemistry 399(7) (2011): 2495-2502.
- [65] Wanigasekara, E., et al. Bonded ionic liquid polymeric material for solid-phase microextraction GC analysis. Analytical and bioanalytical chemistry 396(1) (2010): 511-524.
- [66] Stevenson, F.J. Humus chemistry: genesis, composition, reactions. John Wiley & Sons, 1994.
- [67] Klucakova, M., Pelikan, P., Lapcik, L., Lapcikova, B., Kucerik, J., and Kalab, M. Structure and properties of humic and fulvic acids. I. Properties and reactivity of humic acids and fulvic acids. Journal of Polymer Materials 17(4) (2000): 337-356.
- [68] Perdue, E. Acidic functional groups of humic substances. (1985).
- [69] Davis, T.A., Volesky, B., and Mucci, A. A review of the biochemistry of heavy metal biosorption by brown algae. Water research 37(18) (2003): 4311-4330.
- [70] Fewson, C.A. Humic Substances in Soil, Sediment, and Water. Geochemistry, Isolation, and Characterization: GR Aiken, DM McKnight, RL Wershaw and P. MacCarthy (Editors). Wiley, New York, NY, 1985, xiii+ 692 pp., £ stg. 61.35 (hardcover). 1986, Elsevier.
- [71] de Melo, B.A.G., Motta, F.L., and Santana, M.H.A. Humic acids: Structural properties and multiple functionalities for novel technological developments. Materials Science and Engineering: C 62 (2016): 967-974.
- [72] Mirza, M.A., et al. Role of humic acid on oral drug delivery of an antiepileptic drug. Drug development and industrial pharmacy 37(3) (2011): 310-319.
- [73] Chen, Y. and Stevenson, F. Soil organic matter interactions with trace elements. in The role of organic matter in modern agriculture, pp. 73-116: Springer, 1986.
- [74] Rice-Evans, C., Miller, N., and Paganga, G. Antioxidant properties of phenolic compounds. Trends in plant science 2(4) (1997): 152-159.
- [75] Litvin, V.A. and Minaev, B.F. Spectroscopy study of silver nanoparticles fabrication using synthetic humic substances and their antimicrobial activity.

- Spectrochimica Acta Part A: Molecular and Biomolecular Spectroscopy 108 (2013): 115-122.
- [76] Yates, L.M. and Von Wandruszka, R. Decontamination of polluted water by treatment with a crude humic acid blend. Environmental science & technology 33(12) (1999): 2076-2080.
- [77] Christl, I. and Kretzschmar, R. Relating ion binding by fulvic and humic acids to chemical composition and molecular size. 1. Proton binding. Environmental science & technology 35(12) (2001): 2505-2511.
- [78] Stathi, P. and Deligiannakis, Y. Humic acid-inspired hybrid materials as heavy metal absorbents. Journal of colloid and interface science 351(1) (2010): 239-247.
- [79] Imyim, A., Thanacharupharn, C., Saithongdee, A., Unob, F., and Ruangpornvisuti, V. Simultaneous removal of Ag (I), Cd (II), Cr (III), Ni (II), Pb (II), and Zn (II) from wastewater using humic acid-coated aminopropyl silica gel. Desalination and Water Treatment 57(37) (2016): 17411-17420.
- [80] Tong, Y., Yang, H., Li, J., and Yang, Y. Extraction of Au (III) by ionic liquid from hydrochloric acid medium. Separation and Purification Technology 120 (2013): 367-372.
- [81] Wei, W., Cho, C.-W., Kim, S., Song, M.-H., Bediako, J.K., and Yun, Y.-S. Selective recovery of Au (III), Pt (IV), and Pd (II) from aqueous solutions by liquid-liquid extraction using ionic liquid Aliquat-336. Journal of Molecular Liquids 216 (2016): 18-24.
- [82] Pu, J., Wang, L., Mo, Y., and Xue, Q. Preparation and characterization of ultrathin dual-layer ionic liquid lubrication film assembled on silica surfaces. Journal of colloid and interface science 354(2) (2011): 858-865.
- [83] Marwani, H.M., Alsafrani, A.E., Asiri, A.M., and Rahman, M.M. Silica-gel particles loaded with an ionic liquid for separation of Zr (IV) prior to its determination by ICP-OES. Sensors 16(7) (2016): 1001.
- [84] Vantasin, S., Pienpinijtham, P., Wongravee, K., Thammacharoen, C., and Ekgasit, S. Naked eye colorimetric quantification of protein content in milk

- using starch-stabilized gold nanoparticles. Sensors and Actuators B: Chemical 177 (2013): 131-137.
- [85] Wongravee, K., et al. Chemometric analysis of spectroscopic data on shape evolution of silver nanoparticles induced by hydrogen peroxide. Physical Chemistry Chemical Physics 15(12) (2013): 4183-4189.
- [86] Kaur, A., Goyal, D., and Kumar, R. Surfactant mediated interaction of vancomycin with silver nanoparticles. Applied Surface Science (2017).
- [87] Lu, F., et al. Preparation and characterization of nonaqueous proton-conducting membranes with protic ionic liquids. ACS applied materials & interfaces 5(15) (2013): 7626-7632.
- [88] Link, S. and El-Sayed, M.A. Size and temperature dependence of the plasmon absorption of colloidal gold nanoparticles. The Journal of Physical Chemistry B 103(21) (1999): 4212-4217.
- [89] Farges, F., Sharps, J.A., and Brown Jr, G.E. Local environment around gold (III) in aqueous chloride solutions: An EXAFS spectroscopy study. Geochimica et Cosmochimica Acta 57(6) (1993): 1243-1252.
- [90] Frost, M.S., Dempsey, M., and Whitehead, D.E. The response of citrate functionalised gold and silver nanoparticles to the addition of heavy metal ions. Colloids and Surfaces A: Physicochemical and Engineering Aspects 518 (2017): 15-24.
- [91] Wongmanee, K., Khuanamkam, S., and Chairam, S. Gold nanoparticles stabilized by starch polymer and their use as catalyst in homocoupling of phenylboronic acid. Journal of King Saud University-Science 29(4) (2017): 547-552.
- [92] Bertolini, A. Starches: characterization, properties, and applications. CRC Press, 2009.
- [93] Baruah, B., Craighead, C., and Abolarin, C. One-phase synthesis of surface modified gold nanoparticles and generation of SERS substrate by seed growth method. Langmuir 28(43) (2012): 15168-15176.

- [94] Pastoriza-Santos, I., Pérez-Juste, J., and Liz-Marzán, L.M. Silica-coating and hydrophobation of CTAB-stabilized gold nanorods. Chemistry of Materials 18(10) (2006): 2465-2467.
- [95] Erses, A.S., Fazal, M.A., Onay, T.T., and Craig, W.H. Determination of solid waste sorption capacity for selected heavy metals in landfills. Journal of hazardous materials 121(1-3) (2005): 223-232.
- [96] Lin, T.-L. and Lien, H.-L. Effective and selective recovery of precious metals by thiourea modified magnetic nanoparticles. International journal of molecular sciences 14(5) (2013): 9834-9847.
- [97] Ghazitabar, A., Naderi, M., Ranjbar, R., and Azadmehr, A.-r. Using thiourea ligand of gold-thiourea complex to facilitate direct synthesis of silica@ gold core-shell nanostructures. Journal of the Iranian Chemical Society 12(12) (2015): 2253-2261.
- [98] Uyguner, C.S. and Bekbolet, M. A comparative study on the photocatalytic degradation of humic substances of various origins. Desalination 176(1-3) (2005): 167-176.
- [99] Uyguner, C.S. and Bekbolet, M. Evaluation of humic acid photocatalytic degradation by UV-vis and fluorescence spectroscopy. Catalysis Today 101(3-4) (2005): 267-274.
- [100] Kalin, M., Wheeler, W., and Meinrath, G. The removal of uranium from mining waste water using algal/microbial biomass. Journal of environmental radioactivity 78(2) (2004): 151-177.
- [101] Schmidtchen, F.P. and Berger, M. Artificial organic host molecules for anions. Chemical reviews 97(5) (1997): 1609-1646.
- [102] Jasiorski, M., Łuszczuk, K., and Baszczuk, A. Morphology and absorption properties control of silver nanoparticles deposited on two types of sol-gel spherical silica substrates. Journal of Alloys and Compounds 588 (2014): 70-74.
- [103] Alqadi, M., Noqtah, O.A., Alzoubi, F., Alzoubi, J., and Aljarrah, K. pH effect on the aggregation of silver nanoparticles synthesized by chemical reduction. Materials Science-Poland 32(1) (2014): 107-111.

- [104] Huber, L. Validation and qualification in analytical laboratories. CRC Press, 2007.





APPENDIX

จุฬาลงกรณ์มหาวิทยาลัย
CHULALONGKORN UNIVERSITY

VITA

Miss Pimpimon Anekthirakun was born on July 18, 1983 in Khonkaen, Thailand. She received a Bachelor's degree of Science in Chemistry from Mahidol University in 2006. Subsequently, she received a Master's degree of Science in Chemistry from Chulalongkorn University and a member of Environmental Analysis Research Unit (EARU) under supervision of Associate Professor Dr. Apichat Imyim. She finished her Doctor of Philosophy (Chemistry) in the Academic Year 2018. Her present address is 12/288 Pruksatown Phetkasem 81, Machareon Road, Nongkhaem, Bangkok, Thailand, 10160. Contact number is 089-1502421. Email: pimpimon_a@hotmail.com.

